Advances in Mathematical Physics

Mathematical Foundations of Quantum Mechanics and Quantum Field Theories

Lead Guest Editor: David Carfi
Guest Editors: Alfonso Agnew and Luiz R. Evangelista

Mathematical Foundations of Quantum Mechanics and Quantum Field Theories

Advances in Mathematical Physics

Mathematical Foundations of Quantum Mechanics and Quantum Field Theories

Lead Guest Editor: David Carfì
Guest Editors: Alfonso Agnew and Luiz R. Evangelista

Contents

Hindawi
Advances in Mathematical Physics
Volume 2020, Article ID 8050934, 12 pages
https://doi.org/10.1155/2020/8050934

Research Article

Speech Encryption Algorithm Based on Nonorthogonal Quantum State with Hyperchaotic Keystreams

F. J. Farsana [1] **and K. Gopakumar** [2]

[1]*Electronics and Communication, LBS Centre for Science and Technology, University of Kerala, Kerala, India*
[2]*Electronics and Communication, TKM College of Engineering, Kerala, India*

Correspondence should be addressed to F. J. Farsana; farsanafarooq@gmail.com

Received 8 May 2019; Revised 12 July 2019; Accepted 28 August 2019; Published 14 January 2020

Guest Editor: David Carfì

With the advancement in modern computational technologies like cloud computing, there has been tremendous growth in the field of data processing and encryption technologies. In this contest there is an increasing demand for successful storage of the data in the encrypted domain to avoid the possibility of data breach in shared networks. In this paper, a novel approach for speech encryption algorithm based on quantum chaotic system is designed. In the proposed method, classical bits of the speech samples are initially encoded in nonorthogonal quantum state by the secret polarizing angle. In the quantum domain, encoded speech samples are subjected to bit-flip operation according to the Controlled–NOT gate followed by Hadamard transform. Complete superposition of the quantum state in both Hadamard and standard basis is achieved through Hadamard transform. Control bits for C-NOT gate as well as Hadamard gate are generated with a modified *Lù*-hyperchaotic system. Secret nonorthogonal rotation angles and initial conditions of the hyperchaotic system are the keys used to ensure the security of the proposed algorithm. The computational complexity of the proposed algorithm has been analysed both in quantum domain and classical domain. Numerical simulation carried out based on the above principle showed that the proposed speech encryption algorithm has wider keyspace, higher key sensitivity and robust against various differential and statistical cryptographic attacks.

1. Introduction

1.1. Background. Speech encryption techniques have been widely used in confidential areas such as defence, voice over IP, voice-conferencing, news telecasting, e-commerce etc. In these applications, Integrity protection of the voice data is the major security concern, which demands the development of secure speech cryptographic algorithms. Classical data encryption methods are poorly suited for audio encryption, due to its bulky data capacity, strong correlation between adjacent data samples and the presence of unvoiced data segments. Furthermore, there is no theoretical limit on cloning or copying of data in classical cryptography. Quantum information processing is one of the promising fields of cryptography, in which the fundamental principles of quantum mechanics like Heisenberg uncertainty principle and principle of photon polarization are directly exploited [1]. Any attempt made by an intruder to clone or copy an unknown quantum state will destroy the state and it will be detected [2]. Furthermore, nonorthogonal quantum states cannot be readily distinguished even if the states are known. Quantum cryptography was developed in 1984 by the physicist Charles Henry Bennett and it was experimentally demonstrated in 1992 [3]. In 1982, Richard Feynman introduced the idea of a quantum computer, which uses the basic principles of quantum mechanics to its advantage [4]. Quantum computational model theoretically has high computational power to solve realtime mathematical problems much faster than classical computers [5, 6]. With the development in this field, computationally efficient quantum algorithms like Shores factoring algorithm, Grover's searching algorithm and discrete algorithm have been designed which may threaten classical cryptosystem [6]. Also, quantum signal processing outperforms classical signal processing since quantum Fourier transform [7], quantum discrete cosine transform [8, 9] and quantum wavelet transforms [10] are more efficient than their classical counterparts. Thus, cryptanalysts have to design new algorithms according to the principle of quantum mechanics to protect classical information.

Chaos is another elucidating theory from the field of nonlinear dynamics, which has potential applications in several

functional areas of a digital system such as compression, encryption, and modulation. It is one of the subtle behaviours associated with the evolution of a nonlinear physical system with significant properties such as topological transitivity, aperiodicity, deterministic pseudo randomness, and sensitive dependence on initial conditions [11]. The complex chaos theory have been utilized in many conventional cryptographic approaches like RC5 stream cipher and elliptical curve cryptography to strengthen the security of encryption processes [12, 13]. Cryptographic algorithms based on chaos theory consist of two operations such as permutation and diffusion. In the permutation process data samples in the plaintext is rearranged to destroy the local correlation, making the data unable to understand. While in the diffusion stage data sample is masked by the pseudorandom number generated with the chaotic systems to change the sample values. Amin and Abd El-Latif [14] proposed a secret sharing algorithm, which combines random grids (RG), error diffusion (ED) and chaotic permutation to improve the security. Gopalakrihnan and Ramakrishnan [15] introduced an image encryption algorithm where they adopted multiple chaotic systems such as Logistic-Tent Map (LTM), Logistic-Sin Map (LSM), and Tent-Sin Map (TSM) for intermediate chaotic keystream generation. The reproducibility and deterministic nature of chaotic functions add value to cryptographic processes since the process can be repeated for the same function and same initial conditions. These properties improve the security of the cryptographic process by multiple iterations of chaotic maps based on substitution and diffusion operations [16, 17]. Moreover, S–box generation mechanism based on chaotic function along with substitution and permutation process increases the complexity of the algorithm, consequentially enhances the security [18, 19]. Wang et al. [20] proposed a dynamic keystream selection mechanism for S box generation, which avoids the possibility of the chosen plain text and chosen ciphertext attacks. Data encryption techniques based on a lower dimensional chaotic system have weak resistance to brute force attack, which cannot ensure the security of data due to the small keyspace. To improve the keyspace most of the chaos-based encryption algorithms tend to take advantage of combining more than one chaotic system, but it increases the computational complexity, system resources and time. Consequently, encryption techniques based on hyperchaotic systems have been introduced [21–23]. These systems have more than one positive Lyapunov exponent and rich complex dynamic behaviour. Nonlinear dynamics and fractional order dynamical systems have been widely studied in recent years. Synchronization of fractional order complex dynamical systems has potential applications in secure communication systems. Sheue [24] proposed a speech encryption algorithm based on fractional order chaotic systems. It is based on two-channel transmission method where the original speech is encoded using a nonlinear function of the Lorenz chaotic system. They also, analysed the conditions for synchronization between fractional chaotic systems theoretically by using the Laplace transform.

1.2. Review of Related Works. Quantitative modelling and finite precision realization of nonlinear phenomenon could be easily realized with the development of quantum computational models. Therefore researchers have attempted to combine two fundamental theories of physics like deterministic chaos and probabilistic quantum dynamics to develop new cryptographic algorithms. Vidal et al., introduced an encryption technique, which attributes rich dynamics of hyperchaotic system and some fundamental properties of quantum cryptography [25]. Arnold Cat transform is applied widely as a permutation matrix in several quantum data encryption algorithm [26–29]. Abd El-Latif et al., [26] proposed an image encryption algorithm method where he utilized the concept of toral automorphism, low frequency Y -luminance subband scrambling and quantum chaotic map. In this method discretized quantum chaotic Cat map is employed for substitution by generating an intermediate chaotic key stream. Jiang et al., proposed a quantum image scrambling circuit based on Arnold and Fibonacci transformation [27]. Zhou et al., proposed an algorithm based on double phase random coding and generalized Arnold transform [28], in which image pixels are permuted by the Arnold transform and grey level information is encrypted by the double random-phase process. Akhshani et al., studied the nature of dissipative quantum systems and proposed an image encryption algorithm based on the quantum logistic map [29]. Liang et al., proposed a method, where quantum image is encrypted by XOR operation with C-NOT gate which is controlled by pseudorandom number generated by the Logistic map [30]. Gong et al., introduced an algorithm, in which Chen hyperchaotic system is utilized to control the C-NOT operation [31], where the grey level information is encoded by quantum XOR operation. Later, Li et al., [32] designed a quantum colour image encryption based on multiple discrete chaotic systems where Logistic map, Asymmetric Tent map and Logistic Chebyshev map are used to generate control bits. Recently researchers have attempted to develop quantum key distribution in chaotic regime [33, 34].

1.3. Motivation and Objective of the Present Work. Most of the proposed classical encryption methods are flawed by limited keyspace, computational complexity and weak resistance to differential attacks. However, the proposed chaotic-quantum algorithms are computationally efficient and unconditionally secure [26–35]. But they fail to provide complete superposition of quantum states in encrypted domain. This paper introduces a speech encryption algorithm in the quantum scenario, where in classical bits are encoded in the nonorthogonal quantum states. Nonorthogonal quantum states are prepared by unitary rotations of the classical bits through secret rotation angles. Then, the encoded qubits are encrypted by controlled-NOT operation followed by Hadamard transform based on the key generated by the hyperchaotic system. Here quantum gates are controlled by the keystreams generated with the four dimensional hyperchaotic system proposed by Zhou and Yang [35] based on 3D Lü system. This proposed algorithm extends the security by encrypting quantum messages in both Standard and Hadamard basis. Both secret rotating angles and initial conditions of the hyperchaotic systems constitute the key, which enlarges the keyspace. The resulting algorithm ensures security against various differential and statistical attacks due to its enlarged keyspace.

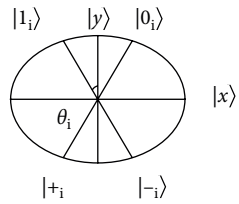

Figure 1: Nonorthogonal quantum pairs.

The rest of this paper is organized as follows: The preliminary study of the proposed speech encryption algorithm is presented in Section 2. Theoretical framework of the proposed approach is given in Section 3. Numerical simulations and performance evaluations are discussed in Section 4. Comparison of the proposed method with other state-of-art is discussed in Section 5, followed by conclusion in Section 6.

2. Preliminary Studies

2.1. Encoding Classical Bits in Nonorthogonal Quantum States. Speech samples are mapped into quantum data media as nonorthogonal quantum state which could be in Standard or Hadamard basis. Figure 1 shows the two pairs of nonorthogonal quantum states in Standard and Hadamard basis. Unlike orthogonal quantum states, nonorthogonal quantum states cannot be discriminated deterministically. Quantum data that encode the classical bits into nonorthogonal quantum states increases the robustness against PNS (photon number splitting) attacks.

Classical bits of the speech samples are encoded in the nonorthogonal quantum state by secret polarizing angle through unitary rotations. Classical binary bit to be encoded in quantum state is $m\{0, 1\}$. Sender encodes the classical bits by choosing nonorthogonal angle θ_i randomly between $[0\ 2\pi]$. The rotation operator $R(\theta_i)$ operates on classical bits m_i results the nonorthogonal quantum states $|m_i\rangle$. Tensor product generates the superposition states $|\psi_m\rangle$ corresponding to $|m_i\rangle$.

The rotation operator in matrix form is expressed by:

$$R(\theta_i) = \begin{bmatrix} \cos\theta_i & \sin\theta_i \\ -\sin\theta_i & \cos\theta_i \end{bmatrix}. \tag{1}$$

In order to retrieve the classical data, the receiver has to rotate the i^{th}quantum bit by the secret angle in the opposite direction. The rotation operator $R(\theta_i)$ is unitary since $R(\theta_i)R^{\dagger}(\theta_i)=\mathbb{I}$, where $R^{\dagger}(\theta_i)$is the adjoint of the matrix and $\mathbb{I}$ is the identity matrix.

$$R(\theta_i)R^{\dagger}(\theta_i) = \begin{bmatrix} \cos^2\theta_i + \sin^2\theta_i & 0 \\ 0 & \cos^2\theta_i + \sin^2\theta_i \end{bmatrix} = \begin{bmatrix} 1 & 0 \\ 0 & 1 \end{bmatrix}. \tag{2}$$

Quantum states corresponding to each classical bit can be expressed as follows:

$$\begin{aligned} |m_1\rangle &= \cos\theta_0|0\rangle + \sin\theta_0|1\rangle, \\ |m_1\rangle &= \cos\theta_0|0\rangle + \sin\theta_0|1\rangle, \\ |m_1\rangle &= \cos\theta_0|0\rangle + \sin\theta_0|1\rangle, \\ |m_1\rangle &= \cos\theta_0|0\rangle + \sin\theta_0|1\rangle, \quad 1 \in [1, n], \end{aligned} \tag{3}$$

where $|m_i\rangle$ is the quantum state corresponding to classical bits m_i for the secret rotation angle θ_i. Tensor product between the quantum states refer to (3) generate the superposition states given as in (4):

$$|\psi_m\rangle = |m_1\rangle \otimes |m_2\rangle \ldots \otimes |m_i\rangle \ldots \otimes |m_n\rangle. \tag{4}$$

Here the n qubit quantum system $|\psi_m\rangle$, exist as the superposition of 2^n states with equal probability.

$$\begin{aligned} |\psi_m\rangle &= \frac{1}{2^n}\sum_{i=0}^{2^n-1} |\psi_{m_i}\rangle \quad i \in [0, 2^n - 1], \\ |\psi_m\rangle &= |0_1 0_2 \ldots 0_n\rangle + |0_1 0_2 \ldots 1_n\rangle \ldots + |\ldots + |1_1 1_2 \ldots 1_n\rangle|. \end{aligned} \tag{5}$$

Superposition states for a three qubit quantum system is described as follows:

$$\begin{aligned} |\psi_m\rangle = |0_1 0_2 0_3\rangle + 0_1 0_2 1_3\rangle + 0_1 1_2 0_3\rangle + |0_1 1_2 1_3\rangle + |1_1 0_2 0_3\rangle \\ + 1_1 0_2 1_3 + |1_1 1_2 0_3\rangle + |1_0 1_1 1_3\rangle. \end{aligned} \tag{6}$$

2.2. Quantum Gates. Quantum gates are the basic tool for quantum information processing. It can be represented as unitary matrix of size $2^n \times 2^n$, if the quantum logic gates acts on a n qubit quantum system. A suitable network of quantum gates can process quantum information much faster than the corresponding classical networks. In the proposed algorithm, quantum gates like Controlled-NOT (C-NOT) gates and Hadamard gates are used.

2.2.1. Controlled-NOT Gate. Controlled-NOT (C-NOT) is the classical counter part of XOR gate. It has two input bits, one control bit and one target bit. If the control bit is set to $|1\rangle$, the gate flips the target qubit. If the control bit is set to $|0\rangle$ target qubit remains same. Mathematical expression of the Controlled-NOT gate can be given as follows:

$$C_{x,y}|x\rangle|y\rangle \rightarrow |x\rangle|x \oplus y\rangle \text{ with } x, y \in \{0, 1\}. \tag{7}$$

CNOT $= \begin{bmatrix} \mathbb{I} & 0 \\ 0 & X \end{bmatrix}$ is the matrix form of CNOT gate, where $\mathbb{I} = \begin{bmatrix} 1 & 0 \\ 0 & 1 \end{bmatrix}$ & $X = \begin{bmatrix} 0 & 1 \\ 1 & 0 \end{bmatrix}$.

2.2.2. Hadamard Gate. In Hadamard basis qubit can be represented as $\{|+\rangle, |-\rangle\}$, which gives the sense of complete superposition between ground state $|0\rangle$ and excited state $|1\rangle$.

$$\begin{aligned} |+\rangle &= \frac{1}{\sqrt{2}}(|0\rangle + |1\rangle), \\ |-\rangle &= \frac{1}{\sqrt{2}}(|0\rangle + |1\rangle). \end{aligned} \tag{8}$$

Hadamard gate operation on single qubit operation is given by:

$$H = \frac{1}{\sqrt{2}}\begin{bmatrix} 1 & 1 \\ 1 & -1 \end{bmatrix} = \frac{1}{\sqrt{2}}(X + Z), \tag{9}$$

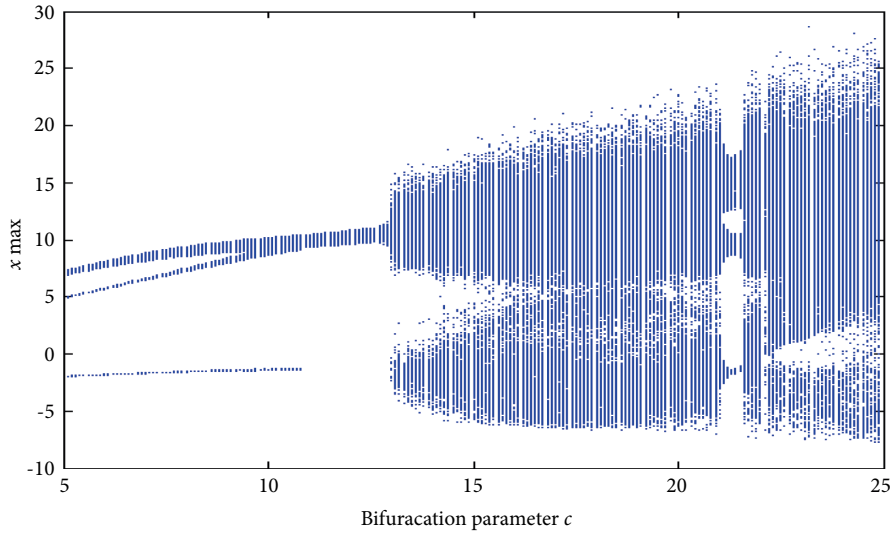

Figure 2: Bifurcation diagram of modified *Lù* system.

where

$$X = \begin{bmatrix} 0 & 1 \\ 1 & 0 \end{bmatrix} \quad Z = \begin{bmatrix} 1 & 0 \\ 0 & -1 \end{bmatrix}. \tag{10}$$

General operation of Hadamard gate on target qubits, which is both in Standard and Hadamard basis are as follows:

$$H|0\rangle = |+\rangle;\ H|1\rangle = |-\rangle;\ H|+\rangle = |0\rangle;\ H|-\rangle = |1\rangle. \tag{11}$$

2.3. Hyperchaotic System. To improve keyspace and security, hyperchaotic systems are widely used in data encryption systems. In the proposed algorithm, keystream for the encryption process is generated from the 4-D hyperchaotic system discovered by Zhou and Yang by the fourth order Runge-Kutta method. The system is described as follows:

$$\begin{aligned} \dot{x} &= 36(y - x), \\ \dot{y} &= -xz + cy, \\ \dot{z} &= xy - 3z, \\ \dot{w} &= 18x - 0.5w. \end{aligned} \tag{12}$$

It has infinite number of real equilibrium. The system (12) shows multiple dynamic behaviour over a wide range of control parameter c. The evolution of chaotic dynamics such as periodic, quasi periodic and chaotic attractors in this system can be obtained by varying control parameter c [0, 25] by fixing all other parameters constant. When $c \in [13, 25]$ the system generates hyperchaotic attractor and this region is utilized for encryption purpose. The encryption process in higher dimensional space eliminates periodic window problems such as limited chaotic range and nonuniform distribution. Figure 2 illustrates the bifurcation diagram of modified *Lù* system.

3. Proposed Algorithm

3.1. Encryption Process. In this section we systematically demonstrate the various steps in encryption process. Figure 3 illustrates the proposed algorithm.

Step 1. Set the values for initial conditions and system parameter for the hyperchaotic system. Generate four different hyperchaotic sequences by iterating the hyperchaotic system by Runge-Kutta method for $l = 2^n$.

The generated sequences are $\{x_i\}, \{y_i\}, \{z_i\}$, and $\{w_i\} (1 \le i \le l)$.

Step 2. Convert the four hyperchaotic sequences into integer sequences $\{x_i^*\}, \{y_i^*\}, \{z_i^*\}$, and $\{w_i^*\}$ as follows:

$$\begin{aligned} x_i^* &= \left|\text{fix}(x_i - \text{fix}(x_i)) \times 10^{14}\right| \text{mod} 2^n, \\ y_i^* &= \left|\text{fix}(y_i - \text{fix}(y_i)) \times 10^{14}\right| \text{mod} 2^n, \\ z_i^* &= \left|\text{fix}(z_i - \text{fix}(z_i)) \times 10^{14}\right| \text{mod} 2^n, \\ w_i^* &= \left|\text{fix}(w_i - \text{fix}(w_i)) \times 10^{14}\right| \text{mod} 2^n. \end{aligned} \tag{13}$$

Step 3. Generate keystream k_1 & k_2 as control bits for C-NOT operation and Hadamard operation.

Control bits k_1 for CNOT operation is given by:

$$\begin{aligned} k_1 &= z_i^n, z_i^{n-1} \ldots z_i^0, \quad z_i^j \in \{0, 1\}, \\ i &= 0, 1, \ldots, 2^n - 1, \quad j = 0, 1, \ldots n. \end{aligned} \tag{14}$$

Control bits k_2 for Hadamard transform is given by:

$$\begin{aligned} k_2 &= w_i^n, w_i^{n-1} \ldots w_i^0, \quad w_i^j \in \{0, 1\}, \\ i &= 0, 1, \ldots, 2^n - 1, \quad j = 0, 1, \ldots n. \end{aligned} \tag{15}$$

Step 4. Controlled NOT gate perform bit flip operation on quantum speech sample $|\psi_m\rangle$ according to the control bits k_1.Where k_1 is realized from keystream $z_i^j\{0, 1\}$ generated with hyperchaotic sequence. Construct a C-NOT operator C_{k_1} as follows:

$$C_{K_1} = \begin{cases} I, \text{when} & z_i^j = 0, \\ X, & z_i^j = 1, \end{cases} \tag{16}$$

where X is the bit flip operator, that operates on the quantum state $|\psi_m\rangle$ according to the control bit z_i^j resulting into new state $|\psi_{m_1}\rangle$.

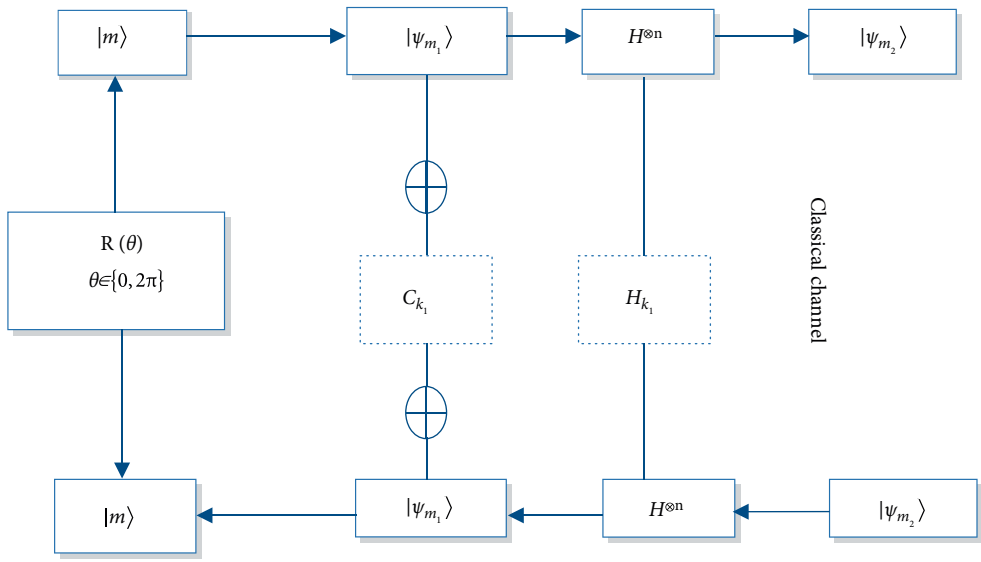

Figure 3: Block diagram of the proposed algorithm.

Table 1: Controlled-NOT operations.

$\lvert\psi_{m_i}\rangle$	C_{K_1}	$\lvert\psi_{m_{1i}}\rangle$
$\lvert\psi_{m_0}\rangle = \lvert 000\rangle$	$\lvert k_{10}\rangle = \lvert 100\rangle$	$\lvert\psi_{m_{10}}\rangle = \lvert 100\rangle$
$\lvert\psi_{m_1}\rangle = \lvert 001\rangle$	$\lvert k_{11}\rangle = \lvert 001\rangle$	$\lvert\psi_{m_{11}}\rangle = \lvert 000\rangle$
$\lvert\psi_{m_2}\rangle = \lvert 001\rangle$	$\lvert k_{12}\rangle = \lvert 110\rangle$	$\lvert\psi_{m_{12}}\rangle = \lvert 100\rangle$
$\lvert\psi_{m_3}\rangle = \lvert 011\rangle$	$\lvert k_{13}\rangle = \lvert 101\rangle$	$\lvert\psi_{m_{13}}\rangle = \lvert 110\rangle$
$\lvert\psi_{m_4}\rangle = \lvert 100\rangle$	$\lvert k_{14}\rangle = \lvert 111\rangle$	$\lvert\psi_{m_{14}}\rangle = \lvert 011\rangle$
$\lvert\psi_{m_5}\rangle = \lvert 101\rangle$	$\lvert k_{15}\rangle = \lvert 011\rangle$	$\lvert\psi_{m_{15}}\rangle = \lvert 110\rangle$
$\lvert\psi_{m_6}\rangle = \lvert 110\rangle$	$\lvert k_{16}\rangle = \lvert 010\rangle$	$\lvert\psi_{m_{16}}\rangle = \lvert 100\rangle$
$\lvert\psi_{m_7}\rangle = \lvert 111\rangle$	$\lvert k_{17}\rangle = \lvert 000\rangle$	$\lvert\psi_{m_{17}}\rangle = \lvert 111\rangle$
$\lvert\psi_{m_0}\rangle = \lvert 000\rangle$	$\lvert k_{10}\rangle = \lvert 100\rangle$	$\lvert\psi_{m_{10}}\rangle = \lvert 100\rangle$

Table 2: Hadamard Transformations.

$\lvert\psi_{m_{1i}}\rangle$	H_{K_2}	$\lvert\psi_{m_{2i}}\rangle$
$\lvert\psi_{m_{10}}\rangle = \lvert 100\rangle$	$\lvert k_{20}\rangle = \lvert 100\rangle$	$\lvert\psi_{m_{20}}\rangle = \lvert -00\rangle$
$\lvert\psi_{m_{11}}\rangle = \lvert 000\rangle$	$\lvert k_{21}\rangle = \lvert 001\rangle$	$\lvert\psi_{m_{21}}\rangle = \lvert 00+\rangle$
$\lvert\psi_{m_{12}}\rangle = \lvert 1000\rangle$	$\lvert k_{22}\rangle = \lvert 110\rangle$	$\lvert\psi_{m_{22}}\rangle = \lvert - + 0\rangle$
$\lvert\psi_{m_{13}}\rangle = \lvert 110\rangle$	$\lvert k_{23}\rangle = \lvert 101\rangle$	$\lvert\psi_{m_{23}}\rangle = \lvert -1+\rangle$
$\lvert\psi_{m_{14}}\rangle = \lvert 011\rangle$	$\lvert k_{24}\rangle = \lvert 111\rangle$	$\lvert\psi_{m_{24}}\rangle = \lvert + - -\rangle$
$\lvert\psi_{m_{15}}\rangle = \lvert 110\rangle$	$\lvert k_{25}\rangle = \lvert 011\rangle$	$\lvert\psi_{m_{25}}\rangle = \lvert 1 - +\rangle$
$\lvert\psi_{m_{16}}\rangle = \lvert 100\rangle$	$\lvert k_{26}\rangle = \lvert 010\rangle$	$\lvert\psi_{m_{26}}\rangle = \lvert 1 + 0\rangle$
$\lvert\psi_{m_{17}}\rangle = \lvert 111\rangle$	$\lvert k_{27}\rangle = \lvert 000\rangle$	$\lvert\psi_{m_{27}}\rangle = \lvert 111\rangle$
$\lvert\psi_{m_{10}}\rangle = \lvert 100\rangle$	$\lvert k_{20}\rangle = \lvert 100\rangle$	$\lvert\psi_{m_{20}}\rangle = \lvert -00\rangle$

$$
\begin{aligned}
\left|\psi_{m_i}\right\rangle &= \frac{1}{2^n}\sum_{i=0}^{2^n-1}\otimes_{j=0}^{j=n}\left|\psi_{m_i}\otimes C_{k_1}\right\rangle,\\
C_{k_1} &= z_i^n, z_i^{n-1}\ldots z_i^0,\ z_i^j \in \{0,1\},\\
\left|\psi_{m_1}\right\rangle &= \frac{1}{2^n}\sum_{i=0}^{2^n-1}\otimes_{j=0}^{j=n}\left|\psi_{m_i}\otimes z_i^j\right\rangle,\\
\left|\psi_{m_1}\right\rangle &= z_i^n, z_i^{n-1}\ldots z_i^0, z_i^j\otimes_{j=0}^{n}\frac{1}{2^n}\sum_{i=0}^{2^n-1}\left|\psi_{m_i}\right\rangle.
\end{aligned}
\tag{17}
$$

Table 1, describe the whole possible quantum states for three qubit system and its C-NOT transformations.

Step 5. Hadamard gate operates on $\left|\psi_{m_1}\right\rangle$ after the bit flip operation performed by Controlled-NOT gate. In this operation k_2 is the control bit and it is realized from keystream $w_i^j\{0,1\}$ generated with the hyperchaotic system. Hadamard gate operates on the target qubit only when the control qubit is $|1\rangle$ or else the target qubit remains the same.

Controlled Hadamard gate operator H_{K_2} is given by:

$$
H_{K_2} = \begin{cases} I, \text{when} & w_i^j = 0,\\ H, & w_i^j = 1. \end{cases}
\tag{18}
$$

Hadamard gate for the n qubit operation

$$
H^{\otimes n} = \frac{1}{\sqrt{2^n}}\sum_{i,j\{0,1\}}(-1)^{ij}.
\tag{19}
$$

Apply Hadamard gate $\left|\psi_{m_i}\right\rangle$ under the control of key element k_2

$$
\left|\psi_{m_2}\right\rangle = \underbrace{\frac{1}{2^n}\sum_{i=0}^{2^n-1}\mathbb{I}\otimes\left|\psi_{m_{1i}}\right\rangle}_{w_i^j=0} + \underbrace{\frac{1}{2^n}\sum_{i=0}^{2^n-1}\rho_{m_{1i}}}_{w_i^j=1}\otimes H^{\otimes n},
\tag{20}
$$

where $\rho_{m_{1i}}$ is the density matrix for the quantum state $\left|\psi_{m_{1i}}\right\rangle$, $\rho_{m_{1i}} = \left|\psi_{m_{1i}}\right\rangle\left\langle\psi_{m_{1i}}\right|$. Hadamard transformation for three qubit system is given in Table 2.

Table 3: Complete operation of four qubit quantum system.

$\lvert\psi_{m_i}\rangle$	C_{K_1}	$\lvert\psi_{m_{1i}}\rangle$	H_{K_2}	$\lvert\psi_{m_{2i}}\rangle$
$\lvert\psi_{m_0}\rangle = \lvert 0000\rangle$	$\lvert k_1\rangle = \lvert 0011\rangle$	$\lvert\psi_{m_{10}}\rangle = \lvert 0011\rangle$	$\lvert k_2\rangle = \lvert 1010\rangle$	$\lvert\psi_{m_{20}}\rangle = \lvert -0+1\rangle$
$\lvert\psi_{m_1}\rangle = \lvert 0001\rangle$		$\lvert\psi_{m_{11}}\rangle = \lvert 0010\rangle$		$\lvert\psi_{m_{21}}\rangle = \lvert -0+0\rangle$
$\lvert\psi_{m_2}\rangle = \lvert 0010\rangle$		$\lvert\psi_{m_{12}}\rangle = \lvert 0001\rangle$		$\lvert\psi_{m_{22}}\rangle = \lvert -0-1\rangle$
$\lvert\psi_{m_3}\rangle = \lvert 0011\rangle$		$\lvert\psi_{m_{13}}\rangle = \lvert 0000\rangle$		$\lvert\psi_{m_{23}}\rangle = \lvert -0-0\rangle$
$\lvert\psi_{m_4}\rangle = \lvert 0100\rangle$		$\lvert\psi_{m_{14}}\rangle = \lvert 0111\rangle$		$\lvert\psi_{m_{24}}\rangle = \lvert -1+1\rangle$
$\lvert\psi_{m_5}\rangle = \lvert 0101\rangle$		$\lvert\psi_{m_{15}}\rangle = \lvert 0110\rangle$		$\lvert\psi_{m_{25}}\rangle = \lvert -1+0\rangle$
$\lvert\psi_{m_6}\rangle = \lvert 0110\rangle$		$\lvert\psi_{m_{16}}\rangle = \lvert 0101\rangle$		$\lvert\psi_{m_{26}}\rangle = \lvert -1-1\rangle$
$\lvert\psi_{m_7}\rangle = \lvert 0111\rangle$		$\lvert\psi_{m_{17}}\rangle = \lvert 0100\rangle$		$\lvert\psi_{m_{27}}\rangle = \lvert -1-0\rangle$
$\lvert\psi_{m_8}\rangle = \lvert 1000\rangle$		$\lvert\psi_{m_{18}}\rangle = \lvert 1011\rangle$		$\lvert\psi_{m_{28}}\rangle = \lvert +0+1\rangle$
$\lvert\psi_{m_9}\rangle = \lvert 1001\rangle$		$\lvert\psi_{m_{19}}\rangle = \lvert 1010\rangle$		$\lvert\psi_{m_{29}}\rangle = \lvert +0+0\rangle$
$\lvert\psi_{m_{10}}\rangle = \lvert 1010\rangle$		$\lvert\psi_{m_{110}}\rangle = \lvert 1001\rangle$		$\lvert\psi_{m_{210}}\rangle = \lvert +0-1\rangle$
$\lvert\psi_{m_{11}}\rangle = \lvert 1011\rangle$		$\lvert\psi_{m_{111}}\rangle = \lvert 1000\rangle$		$\lvert\psi_{m_{211}}\rangle = \lvert +0-0\rangle$
$\lvert\psi_{m_{12}}\rangle = \lvert 1100\rangle$		$\lvert\psi_{m_{112}}\rangle = \lvert 1111\rangle$		$\lvert\psi_{m_{212}}\rangle = \lvert +1+1\rangle$
$\lvert\psi_{m_{13}}\rangle = \lvert 1101\rangle$		$\lvert\psi_{m_{13}}\rangle = \lvert 1110\rangle$		$\lvert\psi_{m_{213}}\rangle = \lvert +1+0\rangle$
$\lvert\psi_{m_{14}}\rangle = \lvert 1110\rangle$		$\lvert\psi_{m_{14}}\rangle = \lvert 1101\rangle$		$\lvert\psi_{m_{214}}\rangle = \lvert +1-1\rangle$
$\lvert\psi_{m_{15}}\rangle = \lvert 1111\rangle$		$\lvert\psi_{m_{15}}\rangle = \lvert 1100\rangle$		$\lvert\psi_{m_{215}}\rangle = \lvert +1-0\rangle$

Detailed encryption process for a four qubit quantum system with fixed $\lvert k_1\rangle = \lvert 0011\rangle$ and $\lvert k_2\rangle = \lvert 1010\rangle$ is given in Table 3.

3.2. Decryption Process. The procedure of decryption process is reverse of the encryption process. Since rotation operator $R(\theta)$, C-NOT gate and H-gate are unitary operators, decryption can be done easily by means of the pre-shared keys. The decryption process is described as follows:

Step 1. Generate the same keystream or control bits k_1 and k_2 according to the steps 1–3 in encryption process.

Step 2. Perform Hadamard operation on $\lvert\psi_{m_2}\rangle$.

$\lvert\psi_{m_1}\rangle = H^{\otimes n}\lvert\psi_{m_2}\rangle$; Since $H^2 = \mathbb{I}$

Step 3. Perform Controlled –NOT operation on $\lvert\psi_{m_2}\rangle$

$$\lvert\psi_m\rangle = \frac{1}{2^n}\sum_{i=0}^{2^n-1}\otimes_{j=0}^{j=n}\lvert\psi_{m_{1i}}\otimes C_{k_1}\rangle. \tag{21}$$

Step 4. Do the inverse rotation operation on $\lvert\psi_m\rangle$ to retrieve the classical data.

4. Numerical Simulation and Results

The proposed algorithm is realized by classical counterpart of circuit elements equivalent to quantum circuit. The proposed algorithm is simulated on a classical computer with MATLAB R2013a (version) software. Eight voice samples of male and female speech signal with sampling rate of 8000 samples/sec are selected for the test. The initial conditions are set as $x0 = 0.423$, $y0 = -0.531$, $z0 = 0.256$, $w0 = 1$. Time step for the fourth order Runge-Kutta method is taken as 0.005.

Table 4: Encrypted signal numerical analysis.

Sample files	*SNR*	Correlation	PRD(Ø)
A. Male voice	−12.45 dB	0.00669	0.521×10^5
B. Female voice	−13.89 dB	0.00918	0.689×10^6
C. Male voice	−21.89 dB	0.00693	0.723×10^5
D. Female voice	−14.32 dB	0.00229	0.214×10^5
E. Male voice	−22.89 dB	0.00527	0.934×10^5
F. Female voice	−19.45 dB	0.00358	0.394×10^6
G. Male voice	−11.76 dB	0.00992	0.861×10^5
H. Female voice	−23.23 dB	0.00136	0.231×10^6

4.1. Correlation Analysis. Correlation analysis is a statistical metric to evaluate the performance of cryptographic algorithm over various statistical attacks. Correlation coefficient analysis measures the mutual relationship between similar segments in the plain audio file and the encrypted audio file. A secure data encryption algorithm converts original data into random-like noisy signal with low correlation coefficient [36]. Low correlation coefficient indicates the narrow correlation between original and encrypted speech files. Correlation

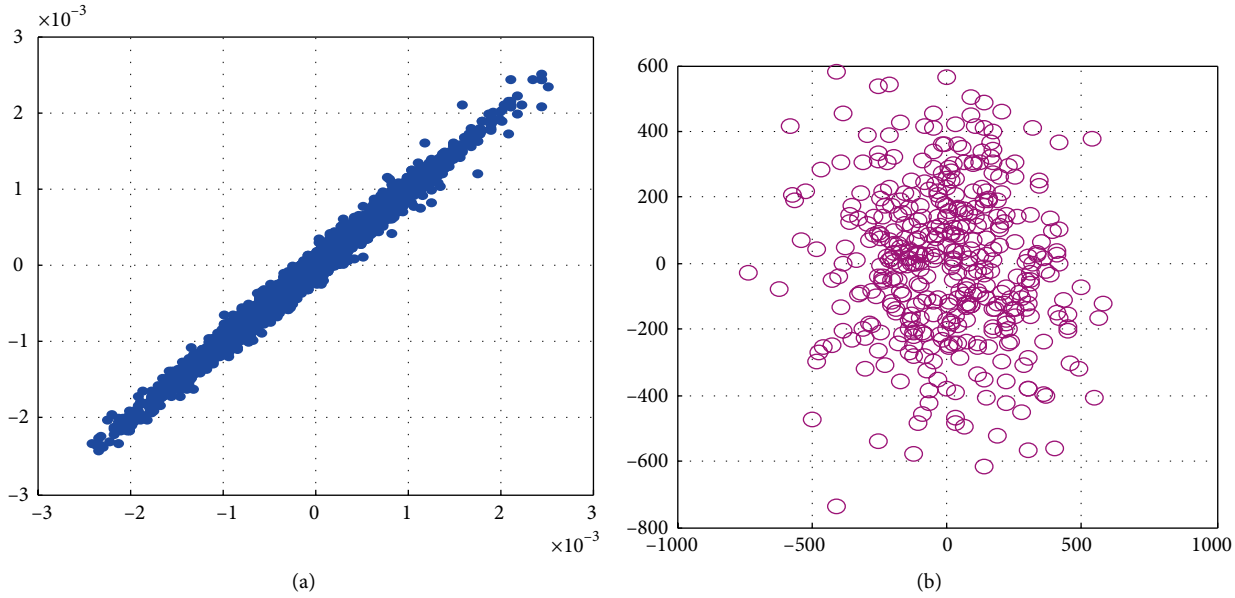

FIGURE 4: Scatter plot diagram of (a) original speech signal (b) encrypted speech signal.

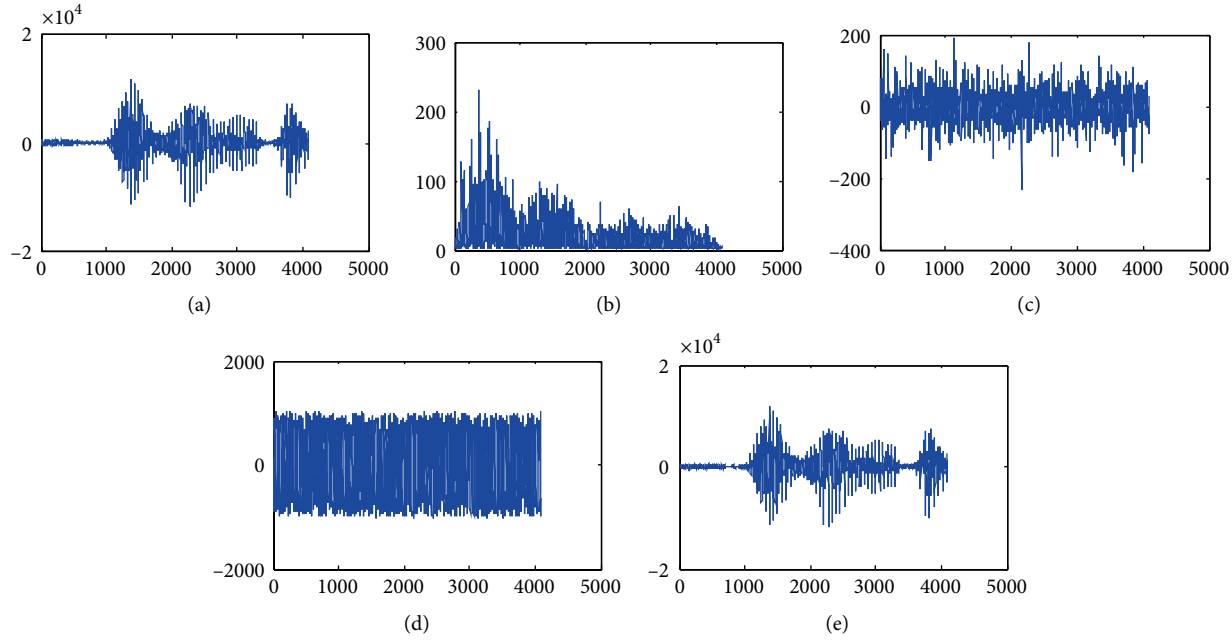

FIGURE 5: (a) Original signal. (b) Compressed signal. (c) Data samples after permutations. (d) Data samples after substitution. (e) Decrypted signal.

coefficient is evaluated based on the equation (22) and it is tabulated in Table 4.

$$r_{xy} = \frac{cov(x,y)}{\sigma_x \sigma_y},$$

$$r_{xy} = \frac{(1/N_S)\sum_{i=1}^{N_s}(x_i - E(x))(y_i - E(y))}{\sqrt{(1/N_S)\sum_{i=1}^{N_s}(x_i - E(x))^2}\sqrt{(i/N_S)\sum_{i=1}^{N_s}(y_i - E(y))^2}}, \sigma_x,$$

$$\sigma_y \neq 0, \tag{22}$$

where $E(x)$ and $E(y)$ are mean and σ_x, σ_y are the standard deviation of the encrypted and decrypted speech signal. Scatter plot diagram is plotted for original and encrypted version, which is shown in Figures 4(a) and 4(b) respectively. It clearly shows that the encrypted version is scattered or randomized.

4.2. Signal to Noise Ratio (SNR). Signal to noise ratio is one of the straight forward methods to validate the performance of data encryption algorithm. SNR measures the noise content in the encrypted data signal. Cryptanalyst always try to increase the noise content in the encrypted signal so as to minimize the information content in the encrypted data [37]. Figure 5 displays the original and encrypted speech signal. It is clear

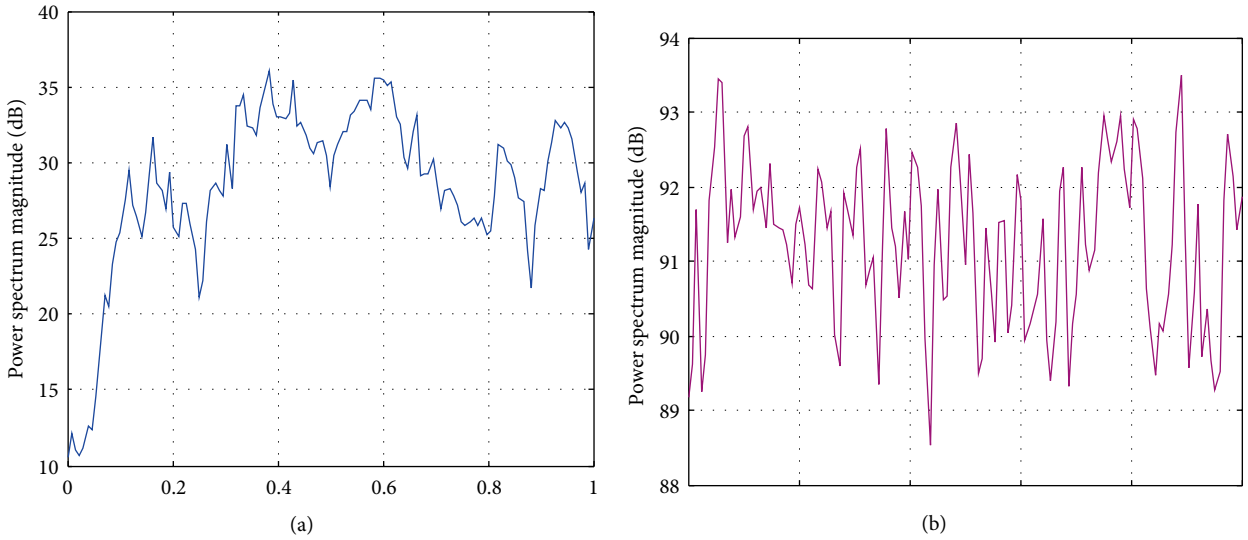

FIGURE 6: Power spectral density of (a) Original speech signal. (b) Encrypted speech signal.

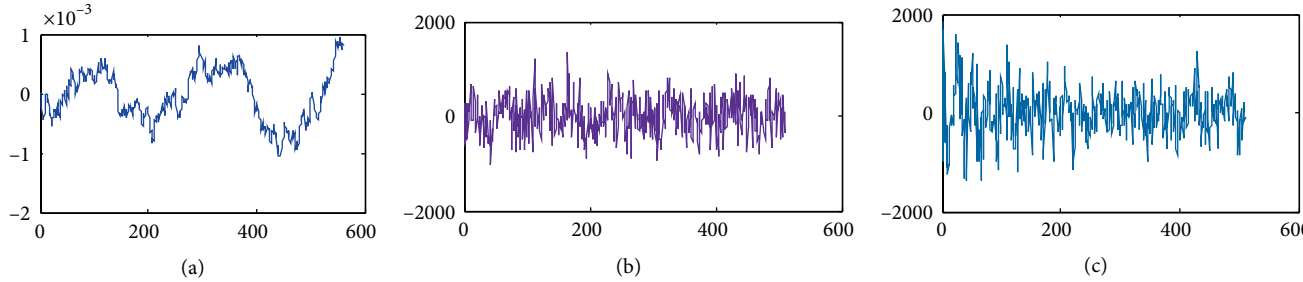

FIGURE 7: Key sensitivity on encryption process (a) original speech signal (b) encrypted speech signal for key $x_0 = 0.413$, $y_0 = -0.931$, $z_0 = 0.465$, $w_0 = 0$ (c) encrypted speech signal for $x_0 = 0.913$, $y_0 = -0.131$, $z_0 = 0$, $w_0 = 0.825$.

that encrypted speech signal contains more noise content that in original speech signal. The SNR values of encrypted audio files are calculated based on the following equation (23) and it is given in Table 4.

$$SNR = 10 * \log 10 \frac{\sum_{i=1}^{N_s} x_i^2}{\sum_{i=1}^{N_s} (x_i - y_i)^2}. \tag{23}$$

4.3. Percent Residual Deviation (PRD). Percentage Residual Deviation is another statistical tool to measure the variation of the encrypted speech signal from original signal. PRD can be calculated for the given plain audio signal x_i and encrypted signal y_i as follows:

$$\emptyset = 100 \times \sqrt{\frac{\sum_{i=1}^{n} (x_i - y_i)^2}{\sum_{i=1}^{n} x_i^2}}. \tag{24}$$

The calculated values of the percent residual deviation for various original and encrypted speech signals are given in Table 4. It can be seen that the encrypted signal is highly deviated from its original signal.

4.4. Spectral Entropy. Spectral entropy measures the randomness in both encrypted and original speech signal. Its measurement is based on the assumption that the spectrum of meaningful speech segment is correlated than the noisy signal. The spectral measurement compares the entropy where the amplitude component of the power spectrum is taken as a probability parameter in entropy calculation. The amount of information can be calculated as the negative of entropy or the negative logarithm of probability. Thus, meaningful speech segments shows low entropy since it contains organized data samples. However the encrypted speech signals have high entropy and large spectral peaks similar to noisy signal. The entropy E_i can be measured as follows:

$$E_i = \sum_n PSD_n(f_i) \log\left(PSD_n(f_i)\right); i = 1, 2, 3 \ldots \ldots, n, \tag{25}$$

where PSD_n is the normalized power spectrum and f_i is the frequency of the signal. Irregularities of amplitude in original and encrypted signals are shown in Figure 6.

4.5. Keyspace and Key Sensitivity Analysis. The secret rotation angles θ_i and initial conditions and system parameter (x_0, y_0, z_0, w_0, c) of the hyperchaotic system determine the keyspace. In the recommended algorithm, floating point accuracy of $10^{-16}$is used for the key components. Therefore the keyspace achieved in this scheme is $\theta_i \times \left(10^{-16}\right)^5 = \theta_i \times 2^{224}$

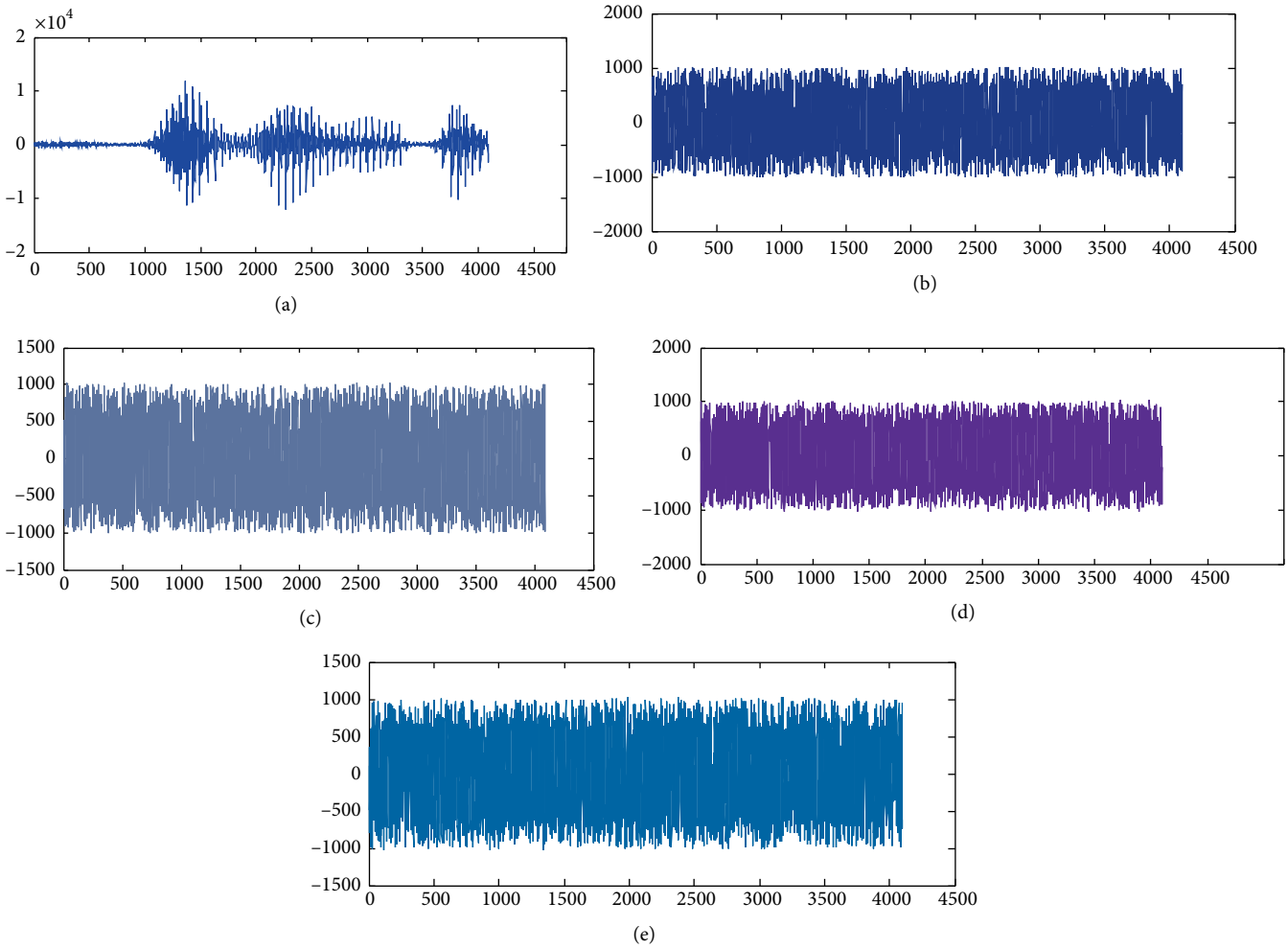

FIGURE 8: Key sensitivity on decryption process (a) decrypted signal with correct key, decrypted signal with incorrect key (b) $x_0 + 10^{-15}$ (c) $y_0 + 10^{-15}$ (d) $z_0 + 10^{-15}$ (e) $w_0 + 10^{-15}$.

TABLE 5: Quality metrics comparison of encryption scheme with other methods.

Method	Key length	keyspace	r_{xy}	NPCR	UACI
AES	128,192,256	$2^{128}, 2^{192}, 2^{256}$	0.009700	99.60327	33.4218
Ref [22]	>264	$>2^{624}$	0.00022	99.6399	33.8085
Ref [23]	744	2^{744}	0.00121	99.6317	33.6781
Ref [26]	$>2^{107}$	2^{107}	0.00321	99.6317	33.6782
[pro:meth]	$>2^{212}$	$> 2^{2^{212}}$	0.000136	99.6320	33.6823

in classical computation. But in the quantum domain the keyspace exist as the superposition of $2^{2^{224}}$ quantum states, which is large enough to break various cryptographic attacks.

Key sensitivity is the essential quality for any good data encryption algorithm, which make sure that the security level of the algorithm against the brute-force attack. It means that a small variation for any key parameters bring an apparent change in both encrypted and decrypted speech signal. The effect of variation in keyparameter on encryption process is verified by encrypting the signal with slightly different initial conditions. The simulation result shows that the slight variation in keyparameter will result completely different encrypted signal. Figure 7 shows the encrypted signals with two different initial conditions. To evaluate the key sensitivity of decrypted signal, encrypt the speech file with one fixed secret key then decryption is performed with slightly different keys. The resulting speech files decrypted with wrong keys apparently looks different and reveals no information.

Figure 8(a) shows the decrypted speech signal with correct key. Figures 8(b)–8(e) show the decrypted signal with slight variations in the initial conditions.

4.6. UACI and NSCR Analysis. In data encryption process, resistace to differential attacks is generally analyzed through NSCR (number of samples change rate) and UACI (unified average changing intensity) tests. In this analyysis two different speech segments are encrypted with same keystreams,where the original speech segments are differed by one sample space [38]. Then the encrypted speeech segments are compared by the number of sample change rate (NSCR) and the unified average changing intensity (UACI). Both these prameters can be expressed as follows:

$$\begin{aligned} \text{NSCR} &= \sum_i \frac{D_i}{N} \times 100\% \; i = 1, 2 \ldots . N, \\ \text{UACI} &= \frac{1}{N}\left[\frac{\sum_i x_i - x_i'}{65535}\right], \end{aligned} \tag{26}$$

where

$$d_i = \begin{cases} 1, & x_i \neq x_i', \\ 0, & \text{otherwise}, \end{cases} \tag{27}$$

c_i and c_i' denotes the the audio samles at i^{th} position of the encrypted speech samples and N corresponds to the length of the speech segments.The upper-bound for NSCR and UACI are 100% and 33.3% respectively. For a secure encryption scheme these parameters should be close to the upper bound ideal values.

4.7. Computational Complexity. In quantum computation, computational complexity is evaluated by the number of quantum gates employed in encryption process. In the proposed algorithm fundamental quantum gates such as C-NOT gate and Hadamard gates are utilized. Since the computational complexity of the quantum computation is parallel, complexity of the entire encryption process could be obtained by the quantum sub-operations like C_{k_1}(C-NOT operator) and H_{K_2}(Hadamard operator). Assume that the input speech samples are encoded in quantum domain and each sample spaces are in a superposition of $2^n \times 1$ quantum states. In Controlled-NOT operation, $(1/2^n)\sum_{i=0}^{2^n-1} \otimes_{j=0}^{j=n} \left|\psi_{m_i} \otimes C_{k_1}\right\rangle$ each qubit is acted upon by C_{k_1} when z_i^j=1. Quantum XOR operator or bit flip operator C_{k_1} is realized by n-CNOT gate. In these operations each n-CNOT gate can be realized by $4n - 8$ Toffoli gates and each Toffoli gate is equivalent to six Control-not gates. Therefore total elementary gates involved in quantum XOR operation is $24n - 48$. Thus, the computational complexity of the first phase of encryption with C-NOT operator is $O(n)$. The Hadamard gate operation on n qubit system is $H^n = \left(1/\sqrt{2^n}\right)\sum_{i,j\{0,1\}}(-1)^{ij}$. The Hadamard gate can be realized by $XZ^{1/2}$. Pauli X and Pauli Z gates can be decomposed to single Toffoli gate with appropriate control signal. Therefore the basic elementary operation involved in Hadamard gate is $6n + 6n$. In the second phase of encryption process the computational complexity of Hadamard operator H_{K_2} can be approximated to $O(n)$. Since both the operations scales linearly with input n, the computational complexity of entire process is $O(n)$. Comparing with classical speech encryption algorithm, the classical XOR operation could be realized with 2^{2n} XOR operations. Therefore the computational complexity of classical encryption algorithm corresponding to its quantum version is $O(2^n)$.

5. Comparison with Existing Works

The proposed algorithm is compared with existing algorithms in both quantum and classical domain. Various quality metrices such as key length, keyspace NPCR, UACI and correlation coefficient between original and encrypted signals are analysed and tabulated in Table 5.

The size of the proposed method's key space is greater than 2^{224} (Section 4.5). It is clear from the simulation results (Figure 4) that the encrypted speech signal contains more noise content that in the original speech signal. Correlation coefficient (CC) evaluated is almost zero (Table 4) for the proposed algorithm. A standard Encryption Algorithm (AES), a fast colour image encryption algorithm based by hyperchaotic system [22], an algorithm based on hyperchaotic system and S boxes in the form of permutation–substitution network [23], and a colour image encryption based on quantum chaotic system [26] are taken for comparison.

6. Conclusion

In this paper, a new classical data encryption algorithm in quantum domain is proposed. The basic idea behind the security of the proposed algorithm lies in protecting the classical information in the form of nonorthogonal quantum states. Furthermore the Controlled NOT operation and Hadamard operation in quantum domain extends the security of the proposed algorithm. The introduction of modified hyperchaotic *Lù*-system into quantum speech encryption algorithm increases the number of keys and improved the key sensitivity. Various simulations and numerical analysis have been carried on classical computer to evaluate the performance of the algorithm. The simulation results demonstrated that the proposed approach is an excellent choice for classical data encryption in quantum domain.

Data Availability

The data used to support the findings of this study are included within the article.

Conflicts of Interest

The authors declare that there are no conflicts of interest regarding the publication of this paper.

References

[1] C. H. Bennett, F. Bessette, G. Brassard, L. Salvail, and J. Smolin, "Experimental quantum cryptography," *Journal of Cryptology*, vol. 5, no. 1, pp. 3–28, 1992.

[2] W. K. Wootters and W. H. Zurek, "A single quantum cannot be cloned," *Nature*, vol. 299, no. 1, pp. 802–803, 1982.

[3] C. H. Bennett and G. Brassard, "Quantum cryptography: public key distribution and coin tossing," vol. 175, in *Proceedings of the IEEE International Conference on Computers, Systems and Signal Processing*, pp. 175–179, IEEE, Bangalore, 1984.

[4] R. P. Feynman, "Simulating physics with computers," *International Journal of Theoretical Physics*, vol. 21, no. 6/7, pp. 467–488, 1982.

[5] G. Beach, C. Lomont, and C. Cohen, "Quantum image processing (quip)," in *IEEE 32nd Applied Imagery Pattern Recognition Workshop Proceedings*, pp. 39–44, IEEE, Washington, DC, USA, 2003.

[6] M. A. Nielson and I. L. Chuang, *Quantum Computation and Quantum Information*, Cambridge University Press, Cambridge, 2000.

[7] V. Vlatko, B. Adriano, and E. Artur, "Quantum network for elementary arithmetic operation," *Physical Review A*, vol. 54, no. 1, pp. 147–153, 1996.

[8] A. Klappenecker and M. Roetteler, "Discrete cosine transforms on quantum computers," in *IEEER8-EURASIP Symposium on Image and Signal Processing and Analysis (ISPA 01)*, pp. 464–468, IEEE, Pula, Croatia, 2001.

[9] C. Tseng and T. Hwang, "Quantum circuit design of 8×8 discrete cosine transforms using its fast computation flow graph," in *IEEE International Symposium on Circuits and Systems*, pp. 828–831, IEEE, Kobe, Japan, 2005.

[10] A. Fijany and C. P. Williams, "Quantum wavelet transform: fast algorithm and complete circuits," in *Proceedings of International Conference on Quantum Computing Quantum Communications*, ACM, pp. 10–33, London, 1997.

[11] G. Alvarez and S. Li, "Some basic cryptographic requirements for chaos-based cryptosystems," *International Journal of Chaos and Bifurcation*, vol. 16, no. 08, pp. 2129–2151, 2006.

[12] O. S. Faragallah, "An enhanced chaotic key-based RC5 block cipher adapted to image encryption," *International Journal of Electronics*, vol. 99, no. 7, pp. 925–943, 2011.

[13] Z. Liu, T. Xia, and J. Wang, "image encryption technology based on fractional two-dimensional triangle function combination discrete chaotic map coupled with menezes-vanstone elliptic curve cryptosystem," *Discrete Dynamics in Nature and Society*, vol. 2018, Article ID 4585083, 24 pages, 2018.

[14] M. Amin and A.A. Abd El-Latif, "Efficient modified RC5 based on chaos adapted to image encryption," *Journal of Electronic Imaging*, vol. 19, no. 1, p. 013012, 2010.

[15] T. Gopalakrihnan and S. Ramakrishnan, "Chaotic image encryption with hash keying as key generator," *IETE Journal of Research*, vol. 63, no. 2, pp. 172–187, 2016.

[16] F. J. Farsana and K. Gopakumar, "A novel approach for speech encryption: Zaslavsky map as pseudo random number generator," vol. 93, in *Proceedings of International Conference on Advances in Computing and Communications (ICACC)*, pp. 816–823, 2016.

[17] S. J. Sheela, K. V. Suresh, and D. Tandur, "A novel audio cryptosystem using chaotic maps and DNA encoding," *Journal of Computer Networks and Communications*, vol. 2017, Article ID 2721910, 12 pages, 2017.

[18] M. Khan, T. Shah, H. Mahmood, M. A. Gondal, and I. Hussain, "A novel technique for the construction of strong S-boxes based on chaotic Lorenz systems," *Nonlinear Dynamics*, vol. 70, no. 3, pp. 2303–2311, 2012.

[19] M. Khan and Z. Asghar, "A novel construction of substitution box for image encryption applications with Gingerbreadman chaotic map and S8 permutation," *Neural Computing and Applications*, vol. 29, no. 4, pp. 993–999, 2018.

[20] X. Wang, Ü. Çavuşoğlu, S. Kacar et al., "S-box based image encryption application using a chaotic system without equilibrium," *Applied Sciences*, vol. 9, no. 4, p. 781, 2019.

[21] H. Zhu, C. Zhao, and X. Zhang, "A novel image encryption–compression scheme using hyper-chaos and Chinese remainder theorem," *Signal Processing: Image Communication*, vol. 28, no. 6, pp. 670–680, 2013.

[22] B. Norouz and S. Mirzakuchaki, "A fast color image encryption algorithm based on hyper-chaotic system," *Nonlinear Dynamics*, vol. 78, no. 2, pp. 995–1015, 2014.

[23] Y. Liu, X. Tong, and J. Ma, "Image encryption algorithm based on hyperchaotic system and dynamic S-box," *Multimed Tools and Applications*, vol. 75, no. 12, pp. 7739–7759, 2016.

[24] L. J. Sheu, "A speech encryption using fractional chaotic systems," *Nonlinear Dynamics*, vol. 63, no. 6/7, pp. 103–108, 2011.

[25] G. Vidal, M. S. Baptista, and H. Mancini, "Fundamentals of a classical chaos-based cryptosystem with some quantum cryptography features," *International Journal of Bifurcation and Chaos*, vol. 22, no. 10, p. 1250243, 2012.

[26] A. A. Abd El-Latif, L. Li, N. Wang, Q. Han, and X. Niu, "A new approach to chaotic image encryption based on quantum chaotic system, exploiting color spaces," *Signal Processing*, vol. 93, no. 11, pp. 2986–3000, 2013.

[27] N. Jiang, W. Y. Wu, and L. Wang, "The quantum realization of Arnold and Fibonacci image scrambling," *Quantum Information Processing*, vol. 13, no. 5, pp. 1223–1236, 2014.

[28] N. R. Zhou, T. X. Hua, L. H. Gong, D. J. Pei, and Q. H. Liao, "Quantum image encryption based on generalized Arnold transform and double random- phase encoding," *Quantum Information Processing*, vol. 14, no. 4, pp. 1193–1213, 2015.

[29] A. Akhshani, A. Akhavan, and S. C. Lim, "An image encryption scheme based on quantum logistic map," *Communication in Nonlinear Science and Numerical simulations*, vol. 17, pp. 4653–4661, 2012.

[30] H. R. Liang, X. Y. Tao, and N. R. Zhou, "Quantum image encryption based on generalized affine transform and logistic map," *Quantum Information Processing*, vol. 15, no. 7, pp. 2701–2724, 2016.

[31] L. H. Gong, X. H. He, S. Cheng, T. X. Hua, and N. R. Zhou, "Quantum image encryption algorithm based on quantum image XOR operations," *International Journal of Theoretical Physics*, vol. 55, no. 7, pp. 3234–3250, 2016.

[32] L. Li, B. Abd-El-Atty, A.A. Abd El-Latif, and A. Ghoneim, "Quantum color image encryption based on multiple discrete chaotic systems," in *Proceedings of the Federated Conference on Computer Science and Information Systems*, pp. 555–529, IEEE, Prague, Czech Republic, 2017.

[33] M. H. Al Hasani and K. A. Al Naimee, "Impact security enhancement in chaotic quantum cryptography," *Optics & Laser Technology*, vol. 119, p. 105575, 2019.

[34] G. l de Oliveira and R. v Ramos, "Quantum-chaotic cryptography," *Quantum Information Processing*, vol. 17, no. 3, 2018.

[35] P. Zhou and F. Yang, "Hyperchaos, chaos and horseshoe in a 4D nonlinear system with an infinite number of equilibrium points," *Nonlinear Dynamics*, vol. 76, no. 1, pp. 473–480, 2014.

[36] R. Taylor, "Interpretation of the correlation coefficient: a basic review," *Journal of Diagnostic Medical Sonography*, vol. 6, no. 1, pp. 35–39, 1990.

[37] B. T. Bosworth, W. R. Bernecky, J. D. Nickila, B. Adal, and G. D. Carter, "Estimating signal-to-noise ratio (SNR)," *IEEE Journal of Oceanic Engineering*, vol. 33, no. 4, pp. 414–418, 2008.

[38] Y. Wu, J.P. Noonan, and S. Agaian, "NPCR and UACI randomness tests for image encryption," *Cyber Journals: Multidisciplinary Journals in Science and Technology Journal of Selected Areas in Telecommunications (JSAT)*, vol. 1, no. 2, pp. 31–38, 2011.

Hindawi
Advances in Mathematical Physics
Volume 2020, Article ID 2676919, 7 pages
https://doi.org/10.1155/2020/2676919

Research Article

Representation of Manifolds for the Stochastic Swift-Hohenberg Equation with Multiplicative Noise

Yanfeng Guo [1,2] **and Donglong Li** [1]

[1] *School of Science, Guangxi University of Science and Technology, Liuzhou, Guangxi, China 545006*
[2] *School of Mathematics and Physics, China University of Geosciences Wuhan, Wuhan, Hubei, China 430074*

Correspondence should be addressed to Yanfeng Guo; guoyan_feng@163.com

Received 27 August 2019; Revised 11 November 2019; Accepted 21 November 2019; Published 8 January 2020

Guest Editor: David Carfi

Representation of approximation for manifolds of the stochastic Swift-Hohenberg equation with multiplicative noise has been investigated via non-Markovian reduced system. The approximate parameterizations of the small scales for the large scales are given in the process of seeking for stochastic parameterizing manifolds, which are obtained as pullback limits of some backward-forward systems depending on the time-history of the dynamics of the low modes in a mean square sense through the nonlinear terms. When the corresponding pullback limits of some backward-forward systems are efficiently determined, the corresponding non-Markovian reduced systems can be obtained for researching good modeling performances in practice.

1. Introduction

Recently, more and more authors have paid attention to considering the approximation problems of manifolds for the stochastic partial differential equations (SPDEs). For decades, various approximating methods have been given to solve these problems, such as amplitude equations approach [1–4] and the manifolds-based approaches [5–11].

In this paper, approximation of manifolds for the stochastic Swift-Hohenberg equation with multiplicative noise will be investigated in Stratonovich sense [12]. It is well known that there have been some authors to consider the approximation of manifolds in large probability sense [1, 2, 13] and they have obtained some results until now. In addition, approximation in parameterizing manifold for a stochastic Swift-Hohenberg equation with additive noise have been investigated by us in [14]. Furthermore, it is needed to consider the problems in Stratonovich sense. Until now, there have been few consideration from the point of view of approximation in parameterizing manifold under the pathwise sense for the stochastic Swift-Hohenberg equation with multiplicative noise. The ideas in [14] can be used to consider the approximation of manifold for some stochastic equations with multiplicative noise. Because the different difficulties come from different noise terms, there are some different methods and techniques in studying stochastic equations with multiplicative noise. Here, we investigate the corresponding problems for the stochastic Swift-Hohenberg equation with multiplicative noise with pathwise and obtain some new results for it. The results obtained in this paper are different from those in [14], although there are some similar sentences in some manuscripts. It is well known that various noises cause various stochastic processes for stochastic equations with different noises. The main differences from results in [14] are given by some formulas with various mathematics meanings, in which some different stochastic functions are used. Because the different difficulties mainly come from various noise terms, there are some new difficulties coming from the multiplicative noise solved in our manuscript. So, some different techniques are used in studying stochastic equations with multiplicative noise.

We will extend the strategy introduced in [5, 6] to the stochastic Swift-Hohenberg equation [12] with multiplicative noise and obtain the approximation of parameterizing manifolds and corresponding non-Markovian reduced system. The key idea is mainly based on the approximate

parameterizations of the small scales for the large scales via the stochastic parameterizing manifolds. Random manifolds will improve the partial knowledge of the solutions of SPDEs in mean square error, when it is compared with its projection onto the resolved modes. Approximation of parameterizing manifolds can be obtained by representing the modes with high wave numbers as the pullback limit depend on the time-history of the modes with low wave numbers for the corresponding backward-forward systems. Some conditions with nonresonance conditions below are given and weaker than those in the classical stochastic invariant manifold theory (see [7, 15, 16] and references therein). On the base of these approximations of parameterizing manifolds, when the corresponding pullback limits of some backward-forward systems are efficiently determined, the corresponding non-Markovian stochastic reduced systems are given to reach good modeling performances in practice and take the form of stochastic differential equations with random coefficients, which convey memory effects via the history of the Wiener process and arise from the nonlinear interactions between the low modes embedded in the noise bath. These random coefficients show an exponential decay of correlations, whose rate depends explicitly on the gaps of the nonresonance conditions. In fact, it is possible to achieve very good parameterizing quality for the stochastic Swift-Hohenberg equation with multiplicative noise from our results. And the performances from the reduced system can be numerically assessed for a corresponding optimal or suboptimal control problem.

The paper is organized as follows. In Section 2, we give our functional framework, some definitions about parameterizing manifolds and some properties of some stochastic processes being used. We have devoted Section 3 to studying the representation of approximation of parameterizing manifolds as pullback limits of the corresponding backward-forward systems for a stochastic Swift-Hohenberg equation with multiplicative noise. In Section 4, on the basis of the approximation of parameterizing manifolds, the non-Markovian stochastic reduced systems involving random coefficients are obtained for the stochastic Swift-Hohenberg with multiplicative noise.

2. Preliminaries

The functional framework spaces are a pair of Hilbert spaces (H_1, H) such that H_1 is compactly and densely embedded in H. Let $A : H_1 \longrightarrow H$ be a sectorial operator [16] such that $-A$ is stable in the sense that its spectrum satisfies $\mathrm{Re}\,(\sigma(-A)) < 0$. And we consider interpolated spaces H_α between H_1 and H with $\alpha \in [0, 1)$ along with the perturbations of the linear operator $-A$ given by a one parameter family B_λ of bounded linear operators from H_α to H, depending continuously on λ. Define $L_\lambda = -A + B_\lambda$, which maps H_1 into H.

A local stochastic Swift-Hohenberg equation with multiplicative noise in Stratonovich sense [1] is written as follows:

$$\begin{aligned} du &= \left(\lambda u - (1+\Delta)^2 u - u^3\right)dt + \sigma u \circ dW_t \\ &\coloneqq (L_\lambda u + F(u))dt + \sigma u \circ dW_t, \end{aligned} \tag{1}$$

with Dirichlet boundary conditions $u(0, t\,; \omega) = u(l, t\,; \omega) = 0$, $t > 0$ and initial condition $u(x, 0\,; \omega) = u_0(x)$, $x \in (0, l)$, where λ is a parameterizing variable, σ is positive, and u_0 is some appropriate initial datum with $H = L^2(0, l)$ and $H_1 = H^4(0, l) \cap H_0^2(0, l)$; $W(t)$ is a standard real valued one-dimensional Brownian motion [17] with paths in $C_0(\mathbb{R}, \mathbb{R})$; and Ω being endowed with its corresponding Borel σ-algebra $\mathscr{F}$, its filtration $\mathscr{F}_t$, the Wiener measure $\mathbb{P}$.

Let $F(u) = -u^3$, which is a continuous triple nonlinear mapping from H^α into H, where $\alpha > (1/3)$. Obviously, function $F(u)$ is a mapping from H_1 into H. Assume $L_\lambda = -A + B_\lambda$, where $B_\lambda = \lambda$ and $A = (1 + \Delta)^2$ is closed self-adjoint linear operator with dense domain $D(A)$ in $H = L^2(D)$. The operator L_λ is self-adjoint with an orthonormal basis of eigenfunctions $\{e_k = \sqrt{2/l}\,\sin(k\pi x/l)\}_{k\in\mathbb{N}}$ in H with corresponding eigenvalues $\{\beta_k(\lambda) = \lambda - (1 - (k^2\pi^2/l^2))^2\}_{k\in\mathbb{N}}$.

Then, problem (1) can be rewritten as

$$du = (L_\lambda u + F(u))dt + \sigma u \circ dW_t, \tag{2}$$

with initial condition $u(x, 0\,; \omega) = u_0(x)$, $x \in (0, l)$ and Dirichlet boundary conditions $u(0, t\,; \omega) = u(l, t\,; \omega) = 0$, $t > 0$. Now, we investigate the random dynamical systems of system (2) in the sense of parameterizing manifolds in [6, 17]. The stochastic parameterizing manifolds are mainly considered for local stochastic Swift-Hohenberg equation with multiplicative noise (2). Firstly, a stochastic parameterizing manifold $\mathfrak{M}$ is seen as the graph of a random function h^{pm}, which is a mapping from H^c to $H^{\alpha,s}$ and provides approximation parameterizations of the high part $u_s(t, \omega) = P_s u(t, \omega)$ by using of the low part $u_c(t, \omega) = P_c u(t, \omega)$. The scalar Langevin equation,

$$dz + zdt = \sigma dW, \tag{3}$$

is given. A unique stationary solution $z(\theta_t\omega)$ of this equation is called the stationary Ornstein-Uhlenbeck (OU) process. By simply integrating on the both sides of (3), the identity

$$\int_0^t z_\sigma(\theta_s\omega)ds + z_\sigma(\theta_t\omega) = z_\sigma(\omega) + \sigma W_t(\omega), \quad \forall t \in \mathbb{R}, \tag{4}$$

holds, which is important for representation of approximation.

3. Representation of Manifolds with Multiplicative Noise

Making use of the method in [6], we investigate the local stochastic Swift-Hohenberg (equation (2)) with multiplicative noise in Stratonovich sense. One considers the following backward-forward system associated with SPDE (2).

$$d\widehat{u}_c^{(1)} = L_\lambda^c \widehat{u}_c^{(1)} ds + \sigma \widehat{u}_c^{(1)} \circ dW_s, \quad s \in [-T, 0], \tag{5}$$

$$\widehat{u}_c^{(1)}(s, \omega)|_{s=0} = \xi \in H^c, \tag{6}$$

$$d\widehat{u}_s^{(1)} = \left(L_\lambda^s \widehat{u}_s^{(1)} + P_s F\left(\widehat{u}_c^{(1)}(s-T,\omega)\right)\right)ds + \sigma \widehat{u}_s^{(1)} \circ dW_{s-T}, \quad s \in [0,T], \tag{7}$$

$$\widehat{u}_s^{(1)}(s, \theta_{-T}\omega)|_{s=0} = 0, \tag{8}$$

where $L_\lambda^c := P_c L_\lambda$ and $L_\lambda^s := P_s L_\lambda$. From system (5), (6), (7), and (8), we know that the initial value of $\widehat{u}_c^{(1)}$ is represented in fiber ω and the initial value of $\widehat{u}_s^{(1)}$ is prescribed in fiber $\theta_{-T}\omega$.

It is possible to obtain the solution of system (5) and (6) by using a backward-forward integration procedure due to the partial coupling between the equations constituting this system, where $\widehat{u}_c^{(1)}$ forces the evolution equation of $\widehat{u}_s^{(1)}$ but not reciprocally. In addition, since $u_c^{(1)}$ is emanated backward from ξ in H^c and forces the equation ruling the evolution of $\widehat{u}_s^{(1)}$, thus $\widehat{u}_s^{(1)}$ depends naturally on ξ. One emphasizes this dependence as $\widehat{u}_s^{(1)}[\xi]$ in the whole paper.

The nonresonance conditions should be given in following theorem, under which the pullback limit of $\widehat{u}_s^{(1)}[\xi]$ exists. Now, representation of an analytical description of such parameterizing manifolds will be provided. In particularly, it emphasizes the dependence on the part of the noise path of the manifolds.

Theorem 1. *Consider the SPDE (2) in the functional setting of Section 2, with F assumed to be a trilinear function. Let* $\mathcal{J} := \{1, \cdots, m\}$ *with* $m = \dim(H^c)$.

Suppose also $\beta_n(\lambda) < 0$ *for all* $n > m$. *Furthermore, assume that the following nonresonance conditions for all* $(i_1, i_2, i_3) \in \mathcal{J}^3$, $n > m$,

$$\begin{aligned} &\text{if } < F\left(e_{i_1}, e_{i_2}, e_{i_3}\right), e_n > \neq 0, \\ &\text{then } \beta_{i_1} + \beta_{i_2} + \beta_{i_3} - \beta_n > 0 \end{aligned} \tag{9}$$

hold. Then, the pullback limit of the solution $\widehat{u}_s^{(1)}[\xi](T, \theta_{-T}\omega; 0)$ *of (7) and (8) exists and is given by*

$$\begin{aligned} \widehat{h}_\lambda^{(1)}(\xi,\omega) &= \lim_{T\to+\infty} \widehat{u}_s^{(1)}[\xi](T, \theta_{-T\omega}; 0)| \\ &= \int_{-\infty}^{0} e^{-L_\lambda^s \tau + 2\sigma W_\tau(\omega)} P_s F\left(e^{L_\lambda^c \tau}\xi\right) d\tau, \forall \xi \in H^c, \quad \omega \in \Omega, \end{aligned} \tag{10}$$

where $\widehat{u}_c^{(1)}(s, \omega; \xi)$ *is the solution of (5) and (6)*

$$\widehat{u}_c^{(1)}(s,\omega;\xi) = e^{L_\lambda^c s + \sigma W_s(\omega)}\xi. \tag{11}$$

Moreover, $\widehat{h}_\lambda^{(1)}$ *has the following analytic expression:*

$$\begin{aligned} \widehat{h}_\lambda^{(1)}(\xi,\omega) = &\sum_{n=m+1}^{\infty} \sum_{i_1=1}^{m} \sum_{i_2=1}^{m} \sum_{i_3=1}^{m} \xi_{i_1}\xi_{i_2}\xi_{i_3} M_{n,\lambda}^{i_1 i_2 i_3}(\omega) \\ &< F\left(e_{i_1}, e_{i_2}, e_{i_3}\right), \quad e_n > e_n, \end{aligned} \tag{12}$$

where $\xi_i = <\xi, e_i>$, $i = 1, \cdots, m$, *and*

$$\begin{aligned} M_{n,\lambda}^{i_1 i_2 i_3}(\omega) = \int_{-\infty}^{0} e^{\tau} &\left(\beta_{i_1}(\lambda) + \beta_{i_2}(\lambda) + \beta_{i_3}(\lambda) - \beta_n(\lambda)\right) \\ &+ 2\sigma W_\tau(\omega)_{d\tau}. \end{aligned} \tag{13}$$

Proof. Firstly, from (5), (6), (7), and (8), one introduces two processes $u_c^{(1)}$ and $u_s^{(1)}$ for $\widehat{u}_c^{(1)}$ and $\widehat{u}_s^{(1)}$ as follows:

$$\begin{aligned} u_c^{(1)}(s,\omega;\xi) &= e^{-z_\sigma(\theta_s\omega)}\widehat{u}_c^{(1)}\left(s,\omega; e^{z_\sigma(\theta_s\omega)}\xi\right), \\ &\qquad s \in [-T, 0], \quad \xi \in H^c, \\ u_s^{(1)}[\xi](s, \theta_{-T}\omega; 0) &= e^{-z_\sigma(\theta_{s-T}\omega)}\widehat{u}_s^{(1)}\left[e^{z_\sigma(\omega)}\xi\right](s, \theta_{-T}\omega; 0), \\ &\qquad s \in [0, T]. \end{aligned} \tag{14}$$

Here, via the above transformation processes, the backward-forward system (5), (6), (7), and (8) is transformed into the following system of random differential equations:

$$\frac{du_c^{(1)}}{ds} = L_\lambda^c u_c^{(1)} + z_\sigma(\theta_s\omega)u_c^{(1)}, \quad s \in [-T, 0], \tag{15}$$

$$u_c^{(1)}(s,\omega)|_{s=0} = \xi \in H^c, \tag{16}$$

$$\begin{aligned} \frac{du_s^{(1)}}{ds} = &L_\lambda^s u_s^{(1)} + z_\sigma(\theta_{s-T}\omega)u_s^{(1)} \\ &+ e^{2z_\sigma(\theta_{s-T}\omega)} P_s F\left(u_c^{(1)}(s-T,\omega)\right), \quad s \in [0,T], \end{aligned} \tag{17}$$

$$u_s^{(1)}(s, \theta_{-T}\omega)|_{s=0} = 0. \tag{18}$$

Using the variation of constants method, we can formally obtain the solution of (15) and (16), which is followed by making use of an integration by parts performed to the resulting stochastic convolution terms

$$u_c^{(1)}(s,\omega;\xi) = e^{L_\lambda^c s + \int_0^s z_\sigma(\theta_r\omega)dr}\xi. \tag{19}$$

Similarly, the solution of (17) and (18) can be also obtained at T, which is formed

$$u_s^{(1)}[\xi](T, \theta_{-T}\omega; 0) = \int_{-T}^{0} e^{-\tau L_\lambda^s + 2z_\sigma(\omega)dr + 2\sigma W_\tau(\omega)} P_s F\left(e^{\tau L_\lambda^c}\xi\right) d\tau, \tag{20}$$

where $u_c^{(1)}(\cdot, \omega; \xi)$ is taken as a form of (19). When $T \longrightarrow +\infty$, since condition (9), the limit of (20) exists, which is formed

$$\begin{aligned} h_\lambda^{(1)}(\xi,\omega) &= \lim_{T\to+\infty} u_s^{(1)}[\xi](T, \theta_{-T}\omega; 0) \\ &= \int_{-\infty}^{0} e^{-\tau L_\lambda^s + 2z_\sigma(\omega)dr + 2\sigma W_\tau(\omega)} P_s F\left(e^{\tau L_\lambda^c}\xi\right) d\tau. \end{aligned} \tag{21}$$

Secondly, one investigates the analysis presentation of this limit. Propose that

$$h_\lambda^{(1)}(\xi,\omega)=\sum_{n=m+1}^{\infty}h_\lambda^{(1),n}(\xi,\omega)e_n, \tag{22}$$

where

$$h_\lambda^{(1),n}(\xi,\omega)=\sum_{i_1,i_2,i_3=1}^{m}e^{2z_\sigma(\omega)}\xi_{i_1}\xi_{i_2}\xi_{i_3}M_{n,\lambda}^{i_1i_2i_3}(\omega) \\ <F(e_{i_1},e_{i_2},e_{i_3}),\quad e_n>. \tag{23}$$

Here, $i_j=1,\cdots,m$ and $\xi_{i_j}=<\xi,e_{i_j}>, j=1,2,3,$ and

$$M_{n,\lambda}^{i_1i_2i_3}(\omega)=\int_{-\infty}^{0}e^{\left(\sum_{j=1}^{3}\beta_{1_j}(\lambda)-\beta_n(\lambda)\right)s+2\sigma W_s(\omega)}ds. \tag{24}$$

According to the same assumptions and the inverse transformation, (11) can be immediately obtained from (19), and the analytic expression of $\widehat{h}_\lambda^{(1)}$ has the form of (12).

Furthermore, the approximation $\widehat{h}_\lambda^{(1)}$ can be provided by the above theorem, which constitutes a parameterizing manifold function of SPDE (2). Moreover, the random coefficients $M_{n,\lambda}$ have decaying property of correlations when it is checked by similar calculations performing for the proof of Lemma 5.1 in [6], which are solutions of auxiliary SDEs

$$dM=\left(1-\left(\sum_{j=1}^{3}\beta_{i_j}(\lambda)-\beta_n(\lambda)\right)M\right)dt-\sigma M\circ dW_t. \tag{25}$$

Remark 2. Here, the random coefficients $M_{n,\lambda}^{i_1i_2i_3}(\omega)$ satisfied the stochastic equation (25) and are different from M_i in [14], since the stochastic processes' transformations are various for stochastic equations with multiplicative noises. So, $M_{n,\lambda}^{i_1i_2i_3}(\omega)$ in this paper and M_i in [14] have different representations by formulas. In this paper, the transformations of stochastic processes are more difficult than those in [14]. So, the random coefficients $M_{n,\lambda}^{i_1i_2i_3}(\omega)$ are much more complex than those in [14]. Then, these differences hold in the whole paper.

4. PM-Based Non-Markovian Reduced System with Multiplicative Noise

In this section, the PM-based non-Markovian reduced system of problem (2) is investigated in two cases that are in two subspaces, $H^c=\mathrm{span}\{e_1\}$ or $H^c=\mathrm{span}\{e_1,e_2\}$, respectively.

When one projects (2) into the subspace H_c, it yields that

$$du_c=(L_\lambda^c u_c+P_cF(u_c+u_s))dt+\sigma u\circ dW_t, \tag{26}$$

where $u_c=P_cu$ with P_c being the canonical projector on subspace H^c. By replacing $u_s(t,\omega)=P_su(t,\omega)$ with (12), the pullback limit $\widehat{h}_\lambda^{(1)}(\xi,\theta_t\omega)$, one yields the following reduced system

$$d\xi=\left(L_\lambda^c\xi+P_cF\left(\xi+\widehat{h}_\lambda^{(1)}(\xi,\theta_t\omega)\right)\right)dt+\sigma\xi\circ dW_t, \tag{27}$$

which provides an approximation of the SPDE dynamics projected onto the low modes.

From (12), the random coefficients of $e_i(x)(i=1,2,\cdots)$ contained in the expansion of $\widehat{h}_\lambda^{(1)}$ exhibit the decaying property of correlations. Therefore, extrinsic memory effects in the Stratonovich sense are conveyed by the drift part of (27), making such reduced systems be non-Markovian (see [18, 19]).

The analytic form of $\widehat{h}_\lambda^{(1)}$ from (12) can be used. The nonlinear interactions $F_n^{i_1i_2i_3}=<F(e_{i_1},e_{i_2},e_{i_3}),e_n>$, have the following form. When $m=1$,

$$F_3^{i_1i_2i_3}=\frac{1}{2l},\quad n=3, \\ F_n^{i_1i_2i_3}=0,\quad n=2\quad\text{or}\quad n\geq 4. \tag{28}$$

When $m=2$,

$$F_n^{i_1i_2i_3}=\frac{1}{2l},\quad \textbf{\textit{when}}\quad i_1+i_2+i_3=n\quad\text{or}\quad i_1-i_2-i_3=n, \\ F_n^{i_1i_2i_3}=-\frac{1}{2l},\quad \textbf{\textit{when}}\quad i_1+i_2-i_3=n\quad\text{or}\quad i_1-i_2+i_3=n, \\ F_n^{i_1i_2i_3}=0,\quad n\geq 7. \tag{29}$$

Firstly, we investigate the system in case $m=1$. Since approximation of parameterizing manifolds have been obtained in Section 3, then one yields that

$$\widehat{h}_\lambda^{(1)}(\xi,\omega)=\frac{1}{2l}\xi_1^3M_{3,\lambda}^{111}(\omega)e_3, \tag{30}$$

where $\xi_1=<\xi,e_1>$, and

$$M_{3,\lambda}^{111}(\omega)=\int_{-\infty}^{0}e^{(3\beta_1(\lambda)-\beta_3(\lambda))s+2\sigma W_s(\omega)}ds. \tag{31}$$

In this case, the approximation is simple. However, it is not enough to present the performances of the corresponding dynamics. Furthermore, parameterizing manifolds in two-dimensional case for low mode are considered, which perform more dynamics than in the above case.

Secondly, when $m=2$, then one can obtain the more complex results than in the case of $m=1$.

Here,

$$\begin{aligned}\widehat{h}_{\lambda}^{(1)}(\xi,\omega) &= \sum_{n-m+1}^{\infty}\sum_{i_1,i_2,i_3=1}^{m}\xi_{i_1}\xi_{i_2}\xi_{i_3}M_{n,\lambda}^{i_1i_2i_3}(\omega) < F\left(e_{i_1},e_{i_2},e_{i_3}\right),e_n > e_n \\ &= \frac{1}{2l}\left(\xi_1^3M_{3,\lambda}^{111}-3\xi_1\xi_2^2M_{3,\lambda}^{122}\right)e_3+\frac{3}{2l}\xi_1^2\xi_2M_{4,\lambda}^{112}e_4 \\ &\quad+\frac{3}{2l}\xi_1\xi_2^2M_{5,\lambda}^{122}e_5+\frac{1}{2l}\xi_2^3M_{6,\lambda}^{222}e_6,\end{aligned} \tag{32}$$

where $\xi_1=\langle\xi,e_1\rangle$, $\xi_2=\langle\xi,e_2\rangle$, and

$$\begin{aligned}M_{3,\lambda}^{111}(\omega) &= \int_{-\infty}^{0}e^{(3\beta_1(\lambda)-\beta_3(\lambda))s+2\sigma W_s(\omega)}ds,\ M_{3,\lambda}^{122}(\omega) \\ &= \int_{-\infty}^{0}e^{(\beta_1(\lambda)+2\beta_2(\lambda)-\beta_3(\lambda))s+2\sigma W_s(\omega)}ds, \\ M_{4,\lambda}^{112}(\omega) &= \int_{-\infty}^{0}e^{(2\beta_1(\lambda)+\beta_2(\lambda)-\beta_4(\lambda))s+2\sigma W_s(\omega)}ds, \\ M_{5,\lambda}^{122}(\omega) &= \int_{-\infty}^{0}e^{(\beta_1(\lambda)+2\beta_2(\lambda)-\beta_5(\lambda))s+2\sigma W_s(\omega)}ds,\ M_{6,\lambda}^{222}(\omega) \\ &= \int_{-\infty}^{0}e^{(3\beta_2(\lambda)-\beta_6(\lambda))s+2\sigma W_s(\omega)}ds.\end{aligned} \tag{33}$$

However, it is complex to use directly the analytic formula of $\widehat{h}_{\lambda}^{(1)}$ to obtain the vector $P_cF(\xi+\widehat{h}_{\lambda}^{(1)}(\xi,\theta_t\omega))$ as ξ is various in H^c in spite of any case in fact. So, we can use $\widehat{u}_s^{(1)}[\xi(t,\omega)](t+T,\theta_T\omega;0)$ to take the place of $\widehat{h}_{\lambda}^{(1)}(\xi,\theta_t\omega)$ on the fly along a trajectory $\xi(t,\omega)$ of interest, where $\widehat{u}_s^{(1)}$ is given by integrating on both sides of the backward-forward system (5), (6), (7), and (8), when T is chosen sufficiently large [6]. Then, it is natural to study the reduced system as follows:

$$\begin{aligned}d\xi_t &= \left(L_{\lambda}^c\xi_t+P_cF\left(\xi_t+\widehat{u}_s^{(1)}[\xi(t,\omega)](t+T,\theta_T\omega;0)\right)\right)dt \\ &\quad+\sigma\xi_t\circ dW_t,\ \xi(0,\omega)=\phi,\quad t>0,\end{aligned} \tag{34}$$

where ϕ is appropriately chosen according to the SPDE initial datum and $\widehat{u}_s^{(1)}[\xi(t,\omega)]$ is given from the following system:

$$\begin{aligned}d\widehat{u}_c^{(1)} &= L_{\lambda}^c\widehat{u}_c^{(1)}ds+\sigma\widehat{u}_c^{(1)}\circ dW_s,\ \widehat{u}_c^{(1)}(s,\omega)|_{s=t}=\xi(t,\omega), \\ &\qquad s\in[t-T,t], \\ d\widehat{u}_s^{(1)} &= \left(L_{\lambda}^s\widehat{u}_s^{(1)}+P_sF\left(\widehat{u}_c^{(1)}(s-T,\omega)\right)\right)ds+\sigma\widehat{u}_s^{(1)}\circ dW_{s-T}, \\ &\qquad \widehat{u}_s^{(1)}(s,\theta_{-T}\omega)|_{s=t}=0,\ s\in[t,t+T].\end{aligned} \tag{35}$$

Now, we give the corresponding non-Markovian systems from the above system. Investigating them in two cases $m=1$ and $m=2$.

Firstly, when $m=1$, one denotes $\xi_1(t,\omega)=\xi_1(t,\omega)e_1$, with $\xi_1(t,\omega)=<\xi(t,\omega),e_1>$. Then, the system can be written as in coordinate form

$$\begin{aligned}d\xi_1 &= \beta_1(\lambda)\xi_1-\frac{3}{2l}\left(\xi_1^3-\xi_1^2y_3^{(1)}+\xi_1\left[y_3^{(1)}\right]^2\right)dt+\sigma\xi_1\circ dW_t, \\ &\qquad t>0,\end{aligned} \tag{36}$$

with $\xi_1(0,\omega)=\langle\phi,e_1\rangle$, where $\xi_t=\xi_1(t,\omega)e_1$ and $y_j^{(1)}$, $j=2,\cdots$, are given from the following system:

$$\begin{aligned}dy_1^{(1)} &= \beta_1(\lambda)_{y_1}^{(1)}ds+\sigma y_1^{(1)}\circ dW_s,\quad s\in[t-T,t], \\ dy_2^{(1)} &= \beta_2(\lambda)y_2^{(1)}ds+\sigma y_2^{(1)}\circ dW_{s-T},\quad s\in[t,t+T], \\ dy_3^{(1)} &= \left(\beta_3(\lambda)y_3^{(1)}+\frac{1}{2l}\left[y_1^{(1)}(s-T,\omega)\right]^3\right)ds+\sigma y_3^{(1)}\circ dW_{s-T}, \\ &\qquad s\in[t,t+T], \\ dy_j^{(1)} &= \beta_j(\lambda)y_j^{(1)}ds+\sigma y_j^{(1)}\circ dW_{s-T},\quad s\in[t,t+T],\quad j=4,\cdots,\end{aligned} \tag{37}$$

with $y_1^{(1)}(s,\omega)|_{s=t}=\xi_1(t,\omega)$, $y_j^{(1)}(s,\theta_{-T}\omega)|_{s=t}=0$, $j=2\cdots$.

Secondly, when $m=2$, one denotes $\xi(t,\omega)=\xi_1(t,\omega)e_1+\xi_2(t,\omega)e_2$, with $\xi_i(t,\omega)=<\xi(t,\omega),e_i>$, $i=1,2$. Then, for $t>0$, the corresponding system can be written as in coordinate form

$$\begin{aligned}d\xi_1 &= \left\{\beta_1(\lambda)\xi_1-\frac{3}{2l}\xi_1^3-\frac{3}{l}\xi_1\xi_2^2+\frac{3}{2l}\left(\left(\xi_1^2-\xi_2^2\right)y_3^{(1)}\right.\right. \\ &\quad\left.+2\xi_1\xi_2y_4^{(1)}+\xi_2^2y_5^{(1)}\right)+\frac{3\xi_1}{l}\left(y_3^{(1)}y_5^{(1)}+y_4^{(1)}y_6^{(1)}\right. \\ &\quad\left.-\sum_{i=3}^{6}\left[y_i^{(1)}\right]^2\right)+\frac{3\xi_2}{l}\left(y_3^{(1)}y_6^{(1)}-\sum_{i=4}^{6}y_{i-1}^{(1)}y_i^{(1)}\right) \\ &\quad-\frac{1}{l}\left(\left[y_3^{(1)}\right]^2y_5^{(1)}+2y_3^{(1)}y_4^{(1)}y_6^{(1)}\right) \\ &\quad\left.-\frac{1}{2l}y_3^{(1)}\left(y_3^{(1)}y_5^{(1)}+y_4^{(1)}y_6^{(1)}\right)\right\}dt+\sigma\xi_1\circ dW_t, \\ d\xi_2 &= \left\{\beta_2(\lambda)\xi_1-\frac{3}{l}\xi_1^2\xi_2-\frac{3}{2l}\xi_2^3+\frac{3}{2l}\left(\xi_1^2y_4^{(1)}\right.\right. \\ &\quad\left.+2\xi_1\xi_2\left(-y_3^{(1)}+y_5^{(1)}\right)+\xi_2^2y_6^{(1)}\right) \\ &\quad+\frac{3\xi_1}{l}\left(y_3^{(1)}y_6^{(1)}-\sum_{i=4}^{6}y_{i-1}^{(1)}y_i^{(1)}\right)-\frac{3\xi_2}{l}\sum_{i=3}^{6}\left[y_i^{(1)}\right]^2 \\ &\quad-\frac{3}{2l}\left(\left[y_3^{(1)}\right]^2y_4^{(1)}+2y_3^{(1)}y_4^1y_5^{(1)}+y_3^{(1)}y_5^{(1)}y_6^{(1)}\right. \\ &\quad\left.\left.+\left[y_4^{(1)}\right]^2y_6^{(1)}\right)\right\}dt+\sigma\xi_2\circ dW_t,\end{aligned} \tag{38}$$

with $\xi_1(0,\omega) = \langle \phi, e_1 \rangle$, $\xi_2(0,\omega) = \langle \phi, e_2 \rangle$, where $\xi_t = \xi_1(t,\omega) e_1 + \xi_2(t,\omega) e_2$ and $y_j^{(1)}, j = 3, \cdots$, are given from following system

$$
\begin{aligned}
dy_1^{(1)} &= \beta_1(\lambda) y_1^{(1)} ds + \sigma y_1^{(1)} \circ dW_s, \quad s \in [t-T, t],\\
dy_2^{(1)} &= \beta_2(\lambda) y_2^{(1)} ds + \sigma y_2^{(1)} \circ dW_s, \quad s \in [t-T, t],\\
dy_3^{(1)} &= \left(\beta_3(\lambda) y_3^{(1)} + \frac{1}{2l} \left(\left[y_1^{(1)}(s-T,\omega) \right]^3 \right.\right.\\
&\quad \left.\left. - 3 y_1^{(1)}(s-T,\omega) \left[y_2^{(1)}(s-T,\omega) \right]^2 \right) \right) ds\\
&\quad + \sigma_3 y_3^{(1)} \circ dW_{s-T}, \quad s \in [t, t+T],\\
dy_4^{(1)} &= \left(\beta_4(\lambda) y_4^{(1)} + \frac{3}{2l} \left[y_1^{(1)}(s-T,\omega) \right]^2 y_2^{(1)}(s-T,\omega) \right) ds\\
&\quad + \sigma y_4^{(1)} \circ dW_{s-T}, \quad s \in [t, t+T],\\
dy_5^{(1)} &= \left(\beta_5(\lambda) y_4^{(1)} + \frac{3}{2l} y_1^{(1)}(s-T,\omega) \left[y_2^{(1)}(s-T,\omega) \right] 2 \right) ds\\
&\quad + \sigma y_5^{(1)} \circ dW_{s-T}, \quad s \in [t, t+T],\\
dy_6^{(1)} &= \left(\beta_6(\lambda) y_6^{(1)} + \frac{1}{2l} \left[y_2^{(1)}(s-T,\omega) \right]^3 \right) ds\\
&\quad + \sigma y_6^{(1)} \circ dW_{s-T}, \quad s \in [t, t+T],\\
dy_j^{(1)} &= \beta_j(\lambda) y_j^{(1)} ds + \sigma y_j^{(1)} \circ dW_{s-T}, \quad s \in [t, t+T],\ j = 7, \cdots,
\end{aligned}
\tag{39}
$$

with $y_1^{(1)}(s,\omega)|_{s=t} = \xi_1(t,\omega), y_2^{(1)}(s,\omega)|_{s=t} = \xi_2(t,\omega), y_j^{(1)}(s, \theta_{-T}\omega)|_{s=t} = 0, \ j = 3, \cdots$..

From the above equations, the representations of approximation for manifold and the corresponding reduced non-Markovian systems for stochastic Swift-Hohenberg equation with multiplicative noise are obtained. And the performances given by the above non-Markovian reduced system should have approximate dynamics on the H^c modes in modeling of the pathwise SPDE (2). It is more important that one should give partial dynamics in approximation sense on the H^c modes in modeling of the pathwise SPDEs in practice. The performances from the reduced system may be numerically assessed for a corresponding optimal or suboptimal control problems in the deduced processes. The numerical results will be further shown in the future. The processes deduced in this manuscript offered an idea in order to further investigate the approximation of stochastic manifold for some quantum stochastic equations with multiplicative noise.

Data Availability

Some data and ideas in our previous work in reference [14] were used to support this study.

Conflicts of Interest

The authors declare that they have no conflicts of interest.

Acknowledgments

This research was supported by the National Natural Science Foundation of China (Nos. 11861013 and 11771444), Guangxi Natural Science Foundation (No. 2017GXNSFAA198221), Promotion of the Basic Capacity of Middle and Young Teachers in Guangxi Universities (No. 2017KY0340), the Fundamental Research Funds for the Central Universities, and the China University of Geosciences (Wuhan) (No. 2018061).

References

[1] D. Blömker, M. Hairer, and G. A. Pavliotis, *Stochastic Swift-Hohenberg Equation near a Change of Stability*, 2007.

[2] D. Blömker and W. Wang, "Qualitative properties of local random invariant manifolds for SPDEs with quadratic nonlinearity," *Journal of Dynamics and Differential Equations*, vol. 22, no. 4, pp. 677–695, 2010.

[3] D. Blomker, *Amplitude Equations for Stochastic Partial Differential Equations. Vol.3 of Interdisciplinary Mathematical Sciences*, World Scientific Publishing, Singapore, 2007.

[4] G. Chen, J. Duan, and J. Zhang, "Geometric shape of invariant manifolds for a class of stochastic partial differential equations," *Journal of Mathematical Physics*, vol. 52, no. 7, p. 072702, 2011.

[5] M. D. Chekroun, H. H. Liu, and S. H. Wang, "Non-Markovian reduced systems for stochastic partial differential equations: the additive noise case," https://arxiv.org/abs/1311.3069v1.

[6] M. D. Chekroun, H. H. Liu, and S. H. Wang, *Stochastic Parameterizing Manifolds and Non-Markovian Reduced Equations–Stochastic Manifolds for Nonlinear SPDEs II*, Springer Briefs in Mathematics, Springer-Verlag, New York, NY, USA, 2015.

[7] J. Duan, K. Lu, and B. Schmalfuss, "Invariant manifolds for stochastic differential equations," *Annals of Probability*, vol. 31, pp. 2109–2135, 2003.

[8] J. Duan, K. Lu, and B. Schmalfuss, "Smooth stable and unstable manifolds for stochastic evolutionary equations," *Journal of Dynamics and Differential Equations*, vol. 16, no. 4, pp. 949–972, 2004.

[9] J.-P. Eckmann and C. E. Wayne, "Propagating fronts and the center manifold theorem," *Communications in Mathematical Physics*, vol. 136, no. 2, pp. 285–307, 1991.

[10] H. Fu, X. Liu, and J. Duan, "Slow manifolds for multi-time-scale stochastic evolutionary systems," *Communications in Mathematical Sciences*, vol. 11, no. 1, pp. 141–162, 2013.

[11] X. Sun, J. Duan, and X. Li, "An impact of noise on invariant manifolds in nonlinear dynamical systems," *Journal of Mathematical Physics*, vol. 51, no. 4, p. 042702, 2010.

[12] J. Swift and P. C. Hohenberg, "Hydrodynamic fluctuations at the convective instability," *Physical Review A*, vol. 15, no. 1, pp. 319–328, 1977.

[13] G. Lin, H. Gao, J. Duan, and V. J. Ervin, "Asymptotic dynamical difference between the nonlocal and local Swift-Hohenberg models," *Journal of Mathematical Physics*, vol. 41, no. 4, pp. 2077–2089, 2000.

[14] Y. F. Guo and J. Duan, "Approximation representation of parameterizing manifold and non-Markovian reduced systems for a stochastic Swift-Hohenberg equation," *Applied Mathematics Letters*, vol. 52, pp. 112–117, 2016.

[15] J. Duan and W. Wang, *Effective Dynamics of Stochastic Partial Differential Equations*, Elsevier, London, UK, 2014.

[16] D. Henry, *Geometric Theory of Semilinear Parabolic Equations*, Spinger-Varlag, Berlin, Germany, 1981.

[17] L. Arnold, *Random Dynamical Systems*, Spinger-Verlag, New York, NY, USA, 1998.

[18] M. Hairer, "Ergodic properties of a class of non-Markovian processes," in *Trends in Stochastic Analysis*, vol. 353 of London Mathematical Society Lecture Note Series, , pp. 65–98, Cambridge University Press, 2009.

[19] M. Hairer and A. Ohashi, "Ergodic theory for SDEs with extrinsic memory," *Annals of Probability*, vol. 35, no. 5, pp. 1950–1977, 2007.

Hindawi
Advances in Mathematical Physics
Volume 2019, Article ID 5136758, 7 pages
https://doi.org/10.1155/2019/5136758

Research Article

Some Curvature Properties on Lorentzian Generalized Sasakian-Space-Forms

Rongsheng Ma and Donghe Pei

School of Mathematics and Statistics, Northeast Normal University, Changchun 130024, China

Correspondence should be addressed to Donghe Pei; peidh340@nenu.edu.cn

Received 10 September 2019; Accepted 2 December 2019; Published 19 December 2019

Guest Editor: David Carfi

In this paper, we investigate the Lorentzian generalized Sasakian-space-form. We give the necessary and sufficient conditions for the Lorentzian generalized Sasakian-space-form to be projectively flat, conformally flat, conharmonically flat, and Ricci semisymmetric and their relationship between each other. As the application of our theorems, we study the Ricci almost soliton on conformally flat Lorentzian generalized Sasakian-space-form.

1. Introduction

Gauge theory, as we all know, has a lot of profound intension and it has permeated all aspects of theoretical physics. It will surely guide future developments in theoretical physics. Gauge theory and principal fiber bundle theory are inextricably linked with each other (see [1]). For instance, the field strength $f^{\kappa}_{\mu\nu}$ of gauge theory is exactly the curvature of a manifold (see [2]). So if we know the curvature properties of a manifold, we can get the distribution of field strength $f^{\kappa}_{\mu\nu}$. The purpose of our paper is to clarify the unsteady field around Lorentzian generalized Sasakian-space-forms in view of principal fiber bundle theory.

In differential geometry, the curvature tensor R is very significant to the nature of a manifold. Many other curvature tensor fields defining on the manifold are related with curvature tensor, for instance, Ricci tensor S, scalar curvature r, and conharmonic curvature tensor K. It has been proven that the curvature depends on sectional curvatures entirely. If a manifold is of constant sectional curvature, then we call it a space-form.

For a *Sasakian manifold*, we have the definition of ϕ-sectional curvature and it plays the same role as a sectional curvature. If the ϕ-sectional curvature of a Sasakian manifold is constant, then the manifold is a *Sasakian-space-form* (see [3]). As a generalization of Sasakian-space-form,-*generalized Sasakian-space-form* was introduced and investigated in [4] and the authors also gave some examples. In short, a generalized Sasakian-space-form is an almost contact metric manifold that the curvature tensor R is related with three smooth functions f_1, f_2, and f_3 defined on the manifold.

In [5], the authors defined the *generalized indefinite Sasakian-space-form*. It is the generalized Sasakian-space-form with a semi-Riemannian metric. In this paper, we are most interested in the Lorentzian manifold because it is very useful in Einstein's general relativity. We call it *Lorentzian generalized Sasakian-space-form*, and to make our paper more concise, we will write it as LGSSF for short. We give the necessary and sufficient condition of the LGSSF with the dimension equal to or greater than five to be some certain curvature tensor conditions. We also clarify the necessary and sufficient condition that LGSSF is *Ricci semisymmetric*. It is meaningful to dig into LGSSF satisfying these conditions because we can understand the relationship between the functions f_1, f_2, and f_3 and the curvature properties of the manifold.

Ricci flow is a powerful tool to investigate manifolds. It was first introduced by Hamilton in [6], and he used it to investigate Riemannian manifolds with positive curvature. There are many solutions to Ricci flow, and the *Ricci soliton* is the self-similar solution of it. Physicists are also interested in the Ricci soliton because in physics, it is regarded as a

quasi-Einstein metric. In our paper, we give the Ricci soliton equation as follows:

$$L_W g + 2S = 2\lambda g. \tag{1}$$

In the equation, L_W denotes the Lie derivative, S denotes the Ricci tensor, g denotes the Riemannian metric, and λ is a real scalar. We call it the triple (g, W, and λ) Ricci soliton on the manifold. People can also use the Ricci soliton to study semi-Riemannian manifolds and refer to [7–9] for more details.

In [10], Pigola et al. introduced and studied the *Ricci almost soliton*. They replaced the real scalar λ by a smooth function defining the manifold and called it the triple (g, W, and λ) Ricci almost soliton. In our paper, we apply the Ricci almost soliton to LGSSF, and in consideration of the curvature properties of the manifolds, we get some interesting results.

We organize our paper as follows. In Section 2, readers can get several basic definitions about LGSSF. Sections 3, 4, 5, and 6 are dedicated to showing how a LGSSF can be projectively flat, conformally flat, conharmonically flat, and Ricci semisymmetric. In Section 7, we apply what we get from Sections 3, 4, 5, and 6 to a Ricci almost soliton on LGSSF and give two examples.

We use U, W, V, X, Y, and Z to denote the smooth tangent vector fields on the manifold, and all manifolds and functions mentioned in our paper are smooth.

2. Preliminaries

If a semi-Riemannian manifold M admits a vector field ζ (we call it a *Reeb vector field* or *characteristic vector field*), a 1-form η, and a (1,1) tensor field ϕ satisfying

$$\begin{aligned} \phi\zeta &= 0, \\ \eta \circ \phi &= 0, \\ \phi^2 &= -id + \eta \otimes \zeta, \\ \eta(\zeta) &= 1, \\ \eta(U) &= \varepsilon g(\zeta, U), \\ g(U, W) &= g(\phi U, \phi W) + \varepsilon \eta(U)\eta(W), \end{aligned} \tag{2}$$

where $\varepsilon = g(\zeta, \zeta) = \pm 1$, then we call such a manifold an ε-almost contact metric manifold [11] or almost contact pseudometric manifold [12], and we call it the triple (ϕ, ζ, and η) almost contact structure on the manifold.

If the 2-form $d\eta$ and the metric g satisfy

$$d\eta(U, W) = g(U, \phi W), \tag{3}$$

then the manifold M is a contact pseudometric manifold and the triple (ϕ, ζ, and η) is a contact structure on the manifold.

We define a vector field on the product $\mathbb{R} \times M^{2n+1}$ by $(h(d/dx), U)$; x is the coordinate on $\mathbb{R}$ and h is a C^∞ function on $\mathbb{R} \times M^{2n+1}$. We define an almost complex structure J on $\mathbb{R} \times M^{2n+1}$ by

$$J\left(h\frac{d}{dx}, U\right) = \left(\eta(U)\frac{d}{dx}, \phi U - h\zeta\right), \tag{4}$$

and it is easy to check $J^2 = -id$. Moreover, if J is integrable, then we will say the almost contact structure (ϕ, ζ, and η) is normal (see [3]). We call an ε-normal contact metric manifold an indefinite Sasakian manifold or an ε-Sasakian manifold.

Now we give the definition of the ϕ-sectional curvature. The plane spanned by U and ϕU is called ϕ-section if U is orthogonal to ζ. The ϕ-sectional curvature is the sectional curvature $K(U, \phi U)$. The curvature of an indefinite Sasakian manifold is determined by ϕ-sectional curvatures entirely.

If the ϕ-sectional curvature of an ε-Sasakian manifold is a constant c, then the curvature tensor of the manifold has the following form [13]:

$$\begin{aligned} R(U, W)X = {} & \frac{c+3\varepsilon}{4}\{g(W, X)U - g(U, X)W\} \\ & + \frac{c-\varepsilon}{4}\{g(U, \phi X)\phi W - g(W, \phi X)\phi U \\ & + 2g(U, \phi W)\phi X\} + \frac{c-\varepsilon}{4}\{\eta(U)\eta(X)W \\ & - \eta(W)\eta(X)U + \varepsilon g(U, X)\eta(W)\zeta \\ & - \varepsilon g(W, X)\eta(U)\zeta\}. \end{aligned} \tag{5}$$

In [5], the author replaced the constants with three smooth functions defining the manifold. For an ε-almost contact metric manifold M, if the curvature tensor is given by

$$\begin{aligned} R(U, W)X = {} & f_1\{g(W, X)U - g(U, X)W\} \\ & + f_2\{g(U, \phi X)\phi W - g(W, \phi X)\phi U \\ & + 2g(U, \phi W)\phi X\} + f_3\{\eta(U)\eta(X)W \\ & - \eta(W)\eta(X)U + \varepsilon g(U, X)\eta(W)\zeta \\ & - \varepsilon g(W, X)\eta(U)\zeta\}, \end{aligned} \tag{6}$$

where $f_1, f_2, f_3 \in C^\infty(M)$, then we call M the generalized indefinite Sasakian-space-form.

In our paper, we only focus on the Lorentzian situation: $\varepsilon = -1$ and the index of the metric is one. We call such manifold the Lorentzian generalized Sasakian-space-form, and in our paper, we denote it by $M_1^{2n+1}(f_1, f_2, f_3)$. Because some of the curvature tensor fields we studied are not suitable for three manifolds, in the following, the dimension of LGSSF $M_1^{2n+1}(f_1, f_2, f_3)$ is greater than three, that is, $n > 1$.

For a LGSSF $M_1^{2n+1}(f_1, f_2, f_3)$, we have two useful equations from (6):

$$R(U, W)\zeta = (f_1 + f_3)(\eta(U)W - \eta(W)U), \tag{7}$$

$$R(\zeta, U)W = (f_1 + f_3)(g(U, W)\zeta + \eta(W)U). \tag{8}$$

Lemma 1. *For a LGSSF $M_1^{2n+1}(f_1, f_2, f_3)$, the Ricci tensor S is*

$$S(U, W) = (2nf_1 + 3f_2 + f_3)g(U, W) + (3f_2 - (2n-1)f_3)\eta(U)\eta(W), \tag{9}$$

so the Ricci operator Q and scalar curvature r are

$$QU = (2nf_1 + 3f_2 + f_3)U + ((2n-1)f_3 - 3f_2)\eta(U)\zeta, \tag{10}$$

$$r = 2n(2n+1)f_1 + 6nf_2 + 4nf_3. \tag{11}$$

Proof. As we all know for a semi-Riemannian manifold of dimension n, the Ricci tensor S and the scalar curvature r are

$$S(U, W) = \sum_{i=1}^{n} \varepsilon_i g(R(U, E_i)E_i, W), \qquad r = \sum_{i=1}^{n} \varepsilon_i S(E_i, E_i), \tag{12}$$

where $\{E_i, \cdots, E_n\}$ is a local orthonormal frame field on the manifold and ε_i is the signature of E_i. The curvature tensor of $M_1^{2n+1}(f_1, f_2, f_3)$ is given by (6) and we know $g(U, W) = \sum \varepsilon_i g(U, E_i)g(X, E_i)$, so we can easily get (9), (10), and (11).

We can use warped product to construct LGSSF (see [5]). Let $h > 0$ be a function on $\mathbb{R}$ and $(N^{2n}, J, \text{and } G)$ be an almost complex manifold. Then, the warped product $M = \mathbb{R} \times_h N$ is a LGSSF with the Lorentzian metric given by

$$g_h = -\pi^*(g_{\mathbb{R}}) + (h \circ \pi)^2 \sigma^*(G), \tag{13}$$

where π is the projection from $\mathbb{R} \times N$ to $\mathbb{R}$ and σ is the projection to N. The almost contact structure is

$$\zeta = \frac{\partial}{\partial x}, \qquad \eta(U) = -g_h(U, \zeta), \qquad \phi(U) = (J\sigma_* U)^*. \tag{14}$$

Theorem 2 (see [5]). *Given a generalized complex space-form $N^{2n}(F_1, F_2)$. Then, $M_1^{2n+1}(f_1, f_2, f_3) = \mathbb{R} \times_h N$ is LGSSF, with functions*

$$f_1 = \frac{(F_1 \circ \pi) + h'^2}{h^2}, \qquad f_2 = \frac{F_2 \circ \pi}{h^2}, \qquad f_3 = -\frac{(F_1 \circ \pi) + h'^2}{h^2} + \frac{h''}{h}. \tag{15}$$

3. Projectively Flat Lorentzian Generalized Sasakian-Space-Form

For a $(2n+1)$-dimensional $(n > 1)$ smooth manifold M, the *projective curvature tensorP* is defined by

$$P(U, W)X = \frac{1}{2n}\{S(U, X)W - S(W, X)U\} + R(U, W)X. \tag{16}$$

It is a way to measure whether a manifold is a space-form because if M is projectively flat $(P = 0)$, then it must be of constant curvature and the converse is also true. For more details, readers can refer to [14].

Theorem 3. *A LGSSF $M_1^{2n+1}(f_1, f_2, f_3)(n > 1)$ is projectively flat if and only if $f_2 = f_3 = 0$.*

Proof. Firstly, we suppose that $P(U, W)X = 0$. Put $U = \zeta$ and replace X by ϕX, then equation (16) will be

$$P(\zeta, W)\phi X = \frac{1}{2n}((2n-1)f_3 - 3f_2)g(W, \phi X)\zeta = 0. \tag{17}$$

In consideration of $g(W, \phi X) \neq 0$, we have

$$(2n-1)f_3 - 3f_2 = 0. \tag{18}$$

Then, equation (9) will be

$$S(W, U) = (2nf_1 + 3f_2 + f_3)g(W, U) = 2n(f_1 + f_3)g(W, U). \tag{19}$$

By the above equation, we can write (16) as

$$\begin{aligned} g(P(U, W)X, Z) = f_2\{&g(U, \phi X)g(\phi W, Z) \\ &- g(W, \phi X)g(\phi U, Z) \\ &+ 2g(U, \phi W)g(\phi X, Z)\} \\ &- f_3\{\eta(W)\eta(X)g(U, Z) \\ &- \eta(U)\eta(X)g(W, Z) + \eta(W)\eta(Z)g(U, X) \\ &- \eta(U)\eta(Z)g(W, X) + g(W, X)g(U, Z) \\ &- g(U, X)g(W, Z)\} = 0. \end{aligned} \tag{20}$$

Setting $U = \phi U$ and $W = \phi W$, we have

$$\begin{aligned} g(P(\phi U, \phi W)X, Z) = f_2\{&g(\phi U, \phi X)g(\phi^2 W, Z) \\ &+ 2g(\phi U, \phi^2 W)g(\phi X, Z) \\ &- g(\phi W, \phi X)g(\phi^2 U, Z)\} \\ &+ f_3\{g(\phi U, X)g(\phi W, Z) \\ &- g(\phi W, X)g(\phi U, Z)\} = 0. \end{aligned} \tag{21}$$

Let us denote the orthonormal local basis of TM by $\{e_1, \cdots, e_{2n}, e_{2n+1} = \zeta\}$. Obviously, the signature of the local

basis is $\{+, \cdots, +, -\}$ and we denote it by $\{\varepsilon_1, \cdots, \varepsilon_{2n}, \varepsilon_{2n+1}\}$. Putting $W = e_i$ and $Z = \varepsilon_i e_i$ in the above equation and summing over i, we will have the following equation:

$$(f_3 - (2n+1)f_2)g(\phi U, \phi X) = 0, \tag{22}$$

since $g(\phi U, \phi X) = \sum_{i=1}^{2n+1} \varepsilon_i g(\phi U, e_i) g(\phi X, e_i)$. Because of $g(\phi U, \phi X) \neq 0$, we get

$$f_3 - (2n+1)f_2 = 0. \tag{23}$$

Taking consideration of $(2n-1)f_3 - 3f_2 = 0$ and $n > 1$, we get

$$f_2 = f_3 = 0. \tag{24}$$

Conversely, we suppose that $f_2 = f_3 = 0$ then use (6) and (9), then (16) will be

$$\begin{aligned} P(U, W)X = {} & f_1\{g(U, X)W - g(W, X)U\} \\ & - f_1\{g(U, X)W - g(W, X)U\} = 0. \end{aligned} \tag{25}$$

In order to get the next theorem of our paper, we first introduce the following famous theorem.

Schur.Theorem (see [15]). If $M^n (n \geq 3)$ is a connected semi-Riemannian manifold, and for each $m \in M$, the sectional curvature $K(m)$ is a constant function on the nondegenerate planes in $T_m M$, then $K(m)$ is a constant function on the manifold.

From Theorem 3, we can get if a LGSSF $M_1^{2n+1}(f_1, f_2, f_3)$ is projectively flat, then $K(m) = f_1$. Using Schur.Theorem, we have the following theorem.

Theorem 4. *If a LGSSF $M_1^{2n+1}(f_1, f_2, f_3)(n > 1)$ is projectively flat, then f_1 is a constant function.*

4. Conformally Flat Lorentzian Generalized Sasakian-Space-Form

The *conformal curvature tensor* C is an important curvature tensor for a manifold, apart from the projective curvature tensor. For a $(2n+1)$-dimensional $(n > 1)$ smooth manifold, it is given by

$$\begin{aligned} C(U, W)X = {} & \frac{1}{2n-1}\{S(U, X)W - S(W, X)U \\ & + g(U, X)QW - g(W, X)QU\} \\ & + \frac{r}{2n(2n-1)}\{g(W, X)U - g(U, X)W\} \\ & + R(U, W)X. \end{aligned} \tag{26}$$

Conformal curvature tensor C is the invariant of conformal transformation. In gauge field theory, it is used to classify the regular form of a curvature tensor when $S(e_i, e_j) \neq 0$. If the metric of a manifold is conformally related with a flat metric, then we will say the manifold is conformally flat $(C = 0)$.

Theorem 5. *A LGSSF $M_1^{2n+1}(f_1, f_2, f_3)(n > 1)$ is conformally flat if and only if $f_2 = 0$.*

Proof. From (6), (9), (10), and (11), equation (26) becomes

$$\begin{aligned} C(U, W)X = {} & f_2\{g(X, \phi W)\phi U - g(X, \phi U)\phi W \\ & + 2g(U, \phi W)\phi X\} \\ & - \frac{3}{2n-1} f_2\{g(W, X)U - g(U, X)W \\ & + \eta(W)\eta(X)U - \eta(U)\eta(X)W \\ & + g(U, X)\eta(W)\zeta - g(W, X)\eta(U)\zeta\}. \end{aligned} \tag{27}$$

So if $f_2 = 0$, then C is zero.

Conversely, we suppose that $C(U, W)X = 0$; first, we put $U = \phi W$ in the above equation, then we will have

$$\begin{aligned} C(U, W)X = {} & 3f_2\{g(\phi W, X)W - g(W, X)\phi W \\ & - \eta(W)\eta(X)\phi W - g(\phi W, X)\eta(W)\zeta\} \\ & + (2n-1)f_2\{g(X, \phi W)(-W + \eta(W)\zeta) \\ & + g(W, X)\phi W + \eta(U)\eta(W)\phi W \\ & + 2g(W, W)\phi X + 2\eta(W)\eta(W)\phi X\} \\ = {} & 3f_2 g(\phi W, X)W - 3f_2\eta(W)\eta(X)\phi W \\ & - 3f_2 g(W, X)\phi W \\ & - 3f_2 g(\phi W, X)\eta(W)\zeta(2n-1)f_2 \\ & \cdot \{g(X, \phi W)\eta(W)\zeta - g(X, \phi W)W \\ & + g(W, X)\phi W + \eta(X)\eta(W)\phi W + 2g(W, W) \\ & + 2\eta(W)\eta(W)\phi X\} = 0. \end{aligned} \tag{28}$$

Then, we have

$$\begin{aligned} (n-2)f_2\{g(\phi W, X)W - g(W, X)\phi W - g(X, \phi W)\eta(W)\zeta \\ - \eta(W)\eta(X)\phi W\} - (2n-1)f_2\{\eta(W)\eta(W)\phi X \\ + g(W, W)\phi X\} = 0. \end{aligned} \tag{29}$$

Again we use the local orthonormal basis $\{e_1, \cdots, e_{2n}, e_{2n+1} = \zeta\}$ with signature $\{\varepsilon_1, \cdots, \varepsilon_{2n}, \varepsilon_{2n+1} = \varepsilon\}$; we choose $X = W = e_k (1 \leq k \leq 2n)$, so $g(W, \zeta) = g(X, \zeta) = 0$ and the above equation becomes

$$(n-2)f_2\varepsilon_k\phi e_k + (2n-1)f_2\varepsilon_k\phi e_k = 0, \tag{30}$$

thus, we have

$$(n-1)f_2\phi e_k = 0. \tag{31}$$

Because n is greater than one, we get $f_2 = 0$.

From Theorem 3, we can get the following theorem.

Theorem 6. *If a LGSSF $M_1^{2n+1}(f_1, f_2, f_3)(n > 1)$ is projectively flat, then it is conformally flat.*

5. Conharmonically Flat Lorentzian Generalized Sasakian-Space-Form

The conharmonic transformation is a kind of special conformal transformation. In general, a conformal transformation does not preserve the harmonic function defined on the manifold. In [16], Ishii introduced and studied the conharmonic transformation, which preserved a special kind of harmonic function. He also proved that a manifold could be reduced to a flat space by a conharmonic transformation if and only if the conharmonic curvature tensor K vanished everywhere on the manifold. In other words, the manifold is conharmonically flat ($K = 0$). For a $(2n+1)$-dimensional $(n > 1)$ smooth manifold, the *conharmonic curvature tensorK* is given by

$$K(U, W)X = \frac{1}{2n-1}\{g(U, X)QW - g(W, X)QU + S(U, X)W - S(W, X)U\} + R(U, W)X. \tag{32}$$

Definition 7. A $(2n+1)$-dimensional $(n > 1)$ LGSSF is said to be ζ-conharmonically flat if it satisfies

$$K(U, W)\zeta = 0. \tag{33}$$

Lemma 8. *A LGSSF $M_1^{2n+1}(f_1, f_2, f_3)(n > 1)$ is ζ-conharmonically flat if and only if $(2n+1)f_1 + 3f_2 + 2f_3 = 0$.*

Proof. From (7) and (10), equation (33) becomes

$$\begin{aligned} K(U, W)\zeta &= \frac{1}{2n-1}\{2n(f_1 + f_3)\eta(W)U \\ &\quad - 2n(f_1 + f_3)\eta(U)W \\ &\quad + (2nf_1 + 3f_2 + f_3)\eta(W)U \\ &\quad - (2nf_1 + 3f_2 + f_3)\eta(U)W\} \\ &\quad + (f_1 + f_3)\{\eta(U)W - \eta(W)U\} \\ &= \frac{1}{2n-1}((2n-1)f_1 + 3f_2 + 2f_3)\{\eta(W)U - \eta(U)W\}. \end{aligned} \tag{34}$$

So $M_1^{2n+1}(f_1, f_2, f_3)$ is ζ-conharmonically flat if and only if $(2n+1)f_1 + 3f_2 + 2f_3 = 0$.

From equation (11) and Lemma 8, we have the following theorem.

Theorem 9. *A LGSSF $M_1^{2n+1}(f_1, f_2, f_3)(n > 1)$ is ζ-conharmonically flat if and only if its scalar curvature $r = 0$.*

By Theorem 3 and Lemma 8, we have the following theorem.

Theorem 10. *If a LGSSF $M_1^{2n+1}(f_1, f_2, f_3)(n > 1)$ is ζ-conharmonically flat and projectively flat, then it is a flat manifold.*

We know that being conharmonically flat is the sufficient condition of ζ-conharmonically flat. So we have the following theorem.

Theorem 11. *If a LGSSF $M_1^{2n+1}(f_1, f_2, f_3)(n > 1)$ is conharmonically flat and projectively flat, then it is a flat manifold.*

It is very important for us to know how a LGSSF can be conharmonically flat.

Theorem 12. *A LGSSF $M_1^{2n+1}(f_1, f_2, f_3)(n > 1)$ is conharmonically flat if and only if $f_2 = 0$ and $(2n+1)f_1 + 2f_3 = 0$.*

Proof. Comparing (26) with (32), we can get

$$C(U, W)X = \frac{(2n-1)f_1 + 3f_2 + 2f_3}{2n-1} \cdot \{g(W, X)U - g(U, X)W\} + K(U, W)X. \tag{35}$$

If $f_2 = 0$ and $(2n+1)f_1 + 2f_3 = 0$, then from Theorem 4

$$K(U, W)X = C(U, W)X - \frac{(2n+1)f_1 + 3f_2 + 2f_3}{2n-1} \cdot \{g(W, X)U - g(U, X)W\} = 0. \tag{36}$$

Conversely, if $K(U, W)X = 0$, we know that the conharmonic transformation is a kind of conformal transformation, so if a manifold is conharmonically flat, then it must be conformally flat. In other words, we can get $C(U, W)X = 0$ (equals to $f_2 = 0$) from $K(U, W)X = 0$, that is

$$\begin{aligned} K(U, W)X &= C(U, W)X - \frac{(2n+1)f_1 + 3f_2 + 2f_3}{2n-1} \cdot \{g(W, X)U - g(U, X)W\} \\ &= -\frac{(2n+1)f_1 + 2f_3}{2n-1}\{g(W, X)U - g(U, X)W\} = 0. \end{aligned} \tag{37}$$

We can get $(2n+1)f_1 + 2f_3 = 0$.

Theorem 13. *A LGSSF $M_1^{2n+1}(f_1, f_2, f_3)(n > 1)$ is conharmonically flat if and only if $f_2 = 0$ and scalar curvature $r = 0$.*

6. Ricci Semisymmetric Lorentzian Generalized Sasakian-Space-Form

There are many classes of smooth manifolds such as locally symmetric and Ricci symmetric. A smooth manifold is Ricci semisymmetric when the curvature operator $R(U, W)$ acting on S vanishes identically, that is

$$R(U, W) \cdot S = 0. \tag{38}$$

Theorem 14. *A $(2n+1)$-dimensional $(n>1)$ LGSSF $M_1^{2n+1}(f_1,f_2,f_3)$ is Ricci semisymmetric if and only if $f_1+f_3=0$ or $3f_2=(2n-1)f_3$.*

Proof. First, we suppose that $M_1^{2n+1}(f_1,f_2,f_3)$ is Ricci semisymmetric, that is

$$(R(U,W)\cdot S)(Y,Z) = -S(Y,R(U,W)Z) - S(R(U,W)Y,Z) = 0. \tag{39}$$

Put $U=\zeta$ in the above equation, then we will have

$$S(R(\zeta,W)Y,Z) + S(Y,R(\zeta,W)Z) = 0. \tag{40}$$

Then, using (8), we can get

$$\begin{aligned}(f_1+f_3)\{&g(W,Y)S(\zeta,Z)+\eta(Y)S(W,Z)\\ &+g(W,Z)S(\zeta,Y)+\eta(Z)S(W,Y)\}\\ &=(f_1+f_3)((2n-1)f_3-3f_2)\{-2\eta(Y)\eta(W)\eta(Z)\\ &-\eta(Z)g(W,Y)-\eta(Y)g(W,Z)\}=0.\end{aligned} \tag{41}$$

Again we use the orthonormal basis $\{e_1,\cdots,e_{2n+1}=\zeta\}$ with signature $\{\varepsilon_1,\cdots,\varepsilon_{2n},\varepsilon_{2n+1}=\varepsilon\}$, and this time, in the above equation, we suppose $W=e_i$ and $Z=\varepsilon_i e_i (1\le i\le 2n+1)$, and taking summation over i, we can get

$$2n(f_1+f_3)((2n-1)f_3-3f_2)\eta(Y)=0. \tag{42}$$

Hence, we get $f_1+f_3=0$ or $(2n-1)f_3-3f_2=0$.

Conversely, if $(2n-1)f_3-3f_2=0$, then by direct calculation,

$$\begin{aligned}(R(U,W)\cdot S)(Y,Z) &= -S(Y,R(U,W)Z)-S(R(U,W)Y,Z)\\ &=-(2nf_1+3f_2+f_3)\{g(R(U,W)Z,Y)\\ &\quad+g(R(U,W)Y,Z)\}=0.\end{aligned} \tag{43}$$

If $f_1+f_3=0$, we notice that $\eta(R(U,W)X)=0$, then we will have

$$\begin{aligned}(R(U,W)\cdot S)(Y,Z) &= -S(Y,R(U,W)Z)-S(R(U,W)Y,Z)\\ &=((2n-1)f_3-3f_2)\{g(R(U,W)Z,Y)\\ &\quad+g(R(U,W)Y,Z)\}=0.\end{aligned} \tag{44}$$

Theorem 15. *If a LGSSF $M_1^{2n+1}(f_1,f_2,f_3)(n>1)$ is conharmonically flat and Ricci semisymmetric, then it is a flat manifold.*

Proof. From Theorem 12 and Theorem 14, we know that if a LGSSF is conharmonically flat and Ricci semisymmetric, then we will have $f_2=0$, $(2n+1)f_1+2f_3=0$, and $3f_2=(2n-1)f_3$ or $f_1+f_3=0$. In any case, we get $f_1=f_2=f_3=0$.

Notice that $f_2=f_3=0$ satisfies $(2n-1)f_3-3f_2=0$, so we can get the following theorem.

Theorem 16. *If a LGSSF $M_1^{2n+1}(f_1,f_2,f_3)(n>1)$ is projectively flat, then it is Ricci semisymmetric.*

7. Ricci Almost Soliton on Lorentzian Generalized Sasakian-Space-Form

According to [10], we give the definition of the Ricci almost soliton. For a manifold M, if the metric g, along with a vector field W and a function λ defining on M satisfies

$$L_W g + 2S = 2\lambda g, \tag{45}$$

where L_W denotes the Lie derivative, then we call it the triple (g, W, and λ) Ricci almost soliton on the manifold. If $W=\nabla f$ where $f: M\longrightarrow \mathrm{R}$, then we call it the ($g$, ∇f, and λ) gradient Ricci almost soliton. In this case, we call f the potential function and equation (45) will be

$$S+\mathrm{Hess}(f)=\lambda g. \tag{46}$$

According to [17], we have the following definition.

Definition 17. A vector field W on a LGSSF $M_1^{2n+1}(f_1,f_2,f_3)$ is said to be a conformal vector field on the manifold if it satisfies

$$(L_W g)(V,X) = -2\rho g(V,X). \tag{47}$$

ρ is a smooth function on $M_1^{2n+1}(f_1,f_2,f_3)$.

We apply some of our theorems to the Ricci almost soliton and then give two examples to illustrate the application of the following theorem.

Theorem 18. *Let (g, W, and λ) be a Ricci almost soliton on a conformally flat LGSSF $M_1^{2n+1}(f_1,f_2,f_3)(n>1)$. If W is a conformal vector field, then the manifold is projectively flat, so it is Ricci semisymmetric and Einstein.*

Proof. if W is a conformal vector field, we have equation (47). From (45), we get

$$S=(\rho+\lambda)g. \tag{48}$$

Comparing the above equation with (9), we will have the following equations:

$$\begin{aligned}\rho+\lambda &= 2nf_1+3f_2+f_3,\\ 3f_2-(2n-1)f_3 &= 0.\end{aligned} \tag{49}$$

Because $M_1^{2n+1}(f_1,f_2,f_3)$ is conformally flat, we have $f_2=0$ (Theorem 5). Then,

$$f_2=f_3=0. \tag{50}$$

So $M_1^{2n+1}(f_1, f_2, f_3)$ is projectively flat using Theorem 3, and then it is Ricci semisymmetric using Theorem 16.

From Theorem 4, f_1 is a constant function. So

$$S = (\rho + \lambda)g = 2nf_1 g. \tag{51}$$

$M_1^{2n+1}(f_1, f_2, f_3)$ is Einstein.

Example 19. Let $N^{2n}(-2, 0)(n > 1)$ be a generalized complex space-form, then $M_1^{2n+1} = (-\pi/4, \pi/4) \times_h N$ is LGSSF, where

$$h(t) = \sin t + \cos t, \tag{52}$$

and it is conformally flat. The function $f(t, x) = f(t) = a\int_0^t h(s)ds + b, a, b \in \mathbb{R}$ is a potential function. Set $W = -\nabla f$ and $\lambda(t) = -ah'(t) - 2n$, then we have ($g_h$, W, and λ) a gradient Ricci almost soliton on the manifold. M is projectively flat, Einstein and Ricci semisymmetric.

Example 20. In this instance, we consider the generalized complex space-form $N^{2n}(3, 0)(n > 1)$, and the warped product function h is

$$h(t) = \sinh t + 2\cosh t. \tag{53}$$

The warped product $M_1^{2n+1} = \mathbb{R} \times_h N$ is LGSSF and it is conformally flat.

We have (g_h, W, and λ) a gradient Ricci almost soliton on the manifold that $W = -\nabla f$ and $\lambda(t) = -ah'(t) + 2n$, with $f(t, x) = f(t) = a\int_0^t h(s)ds + b, a, b \in \mathbb{R}$. The manifold is projectively flat, Einstein and Ricci semisymmetric.

8. Conclusion

We present the necessary and sufficient conditions for LGSSF to be projectively flat, conformally flat, conharmonically flat, and Ricci semisymmetric. We also study the Ricci almost soliton on LGSSF. As a result, we know how to construct a Lorentzian manifold with certain curvature tensor conditions, which is useful in gauge theories because of the correspondence between curvature and field strength.

Data Availability

The data used to support the findings of this study are included within the article.

Conflicts of Interest

The authors declare that there are no conflicts of interests in this work.

Acknowledgments

The second author is supported by the National Natural Science Foundation of China (Grant No. 11671070).

References

[1] H. d. A. Gomes, "Classical gauge theory in Riem," *Journal of Mathematical Physics*, vol. 52, no. 8, article 082501, 2011.

[2] T. T. Wu and C. N. Yang, "Concept of nonintegrable phase factors and global formulation of gauge fields," *Physical Review D*, vol. 12, no. 12, pp. 3845–3857, 1975.

[3] D. E. Blair, *Riemannian Geometry of Contact and Symplectic Manifolds, Volume 203 of Progress in Mathematics*, Birkhauser Boston, Inc., Boston, MA, USA, 2nd edition, 2010.

[4] P. Alegre, D. E. Blair, and A. Carriazo, "Generalized Sasakian-space-forms," *Israel Journal of Mathematics*, vol. 141, no. 1, pp. 157–183, 2004.

[5] P. Alegre and A. Carriazo, "Semi-Riemannian generalized Sasakian space forms," *Bulletin of the Malaysian Mathematical Sciences Society*, vol. 41, no. 1, pp. 1–14, 2018.

[6] R. S. Hamilton, "Three-manifolds with positive Ricci curvature," *Journal of Differential Geometry*, vol. 17, no. 2, pp. 255–306, 1982.

[7] W. Batat, M. Brozos-Vázquez, E. García-Río, and S. Gavino-Fernández, "Ricci solitons on Lorentzian manifolds with large isometry groups," *Bulletin of the London Mathematical Society*, vol. 43, no. 6, pp. 1219–1227, 2011.

[8] C. L. Bejan and M. Crasmareanu, "Second order parallel tensors and Ricci solitons in 3-dimensional normal paracontact geometry," *Annals of Global Analysis and Geometry*, vol. 46, no. 2, pp. 117–127, 2014.

[9] G. Calvaruso and A. Zaeim, "A complete classification of Ricci and Yamabe solitons of non-reductive homogeneous 4-spaces," *Journal of Geometry and Physics*, vol. 80, pp. 15–25, 2014.

[10] S. Pigola, M. Rigoli, M. Rimoldi, and A. G. Setti, "Ricci almost solitons," *Annali della Scuola Normale Superiore di Pisa-Classe di Scienze*, vol. 10, no. 4, pp. 757–799, 2011.

[11] K. L. Duggal, "Space time manifolds and contact structures," *International Journal of Mathematics and Mathematical Sciences*, vol. 13, no. 3, pp. 545–553, 1990.

[12] G. Calvaruso and D. Perrone, "Contact pseudo-metric manifolds," *Differential Geometry and its Applications*, vol. 28, no. 5, pp. 615–634, 2010.

[13] R. Kumar, R. Rani, and R. K. Nagaich, "On sectional curvatures of (ε)-Sasakian manifolds," *International Journal of Mathematics and Mathematical Sciences*, vol. 2007, Article ID 93562, 8 pages, 2007.

[14] S. Bochner, "Curvature and Betti numbers," *The Annals of Mathematics*, vol. 49, no. 2, pp. 379–390, 1948.

[15] B. O'Neill, *Semi-Riemannian Geometry: With Applications to Relativity*, Academic Press, 1983.

[16] Y. Ishii, "On conharmonic transformations," *The Tensor Society Tensor New Series*, vol. 7, pp. 73–80, 1957.

[17] G. S. Hall and J. D. Steele, "Conformal vector fields in general relativity," *Journal of Mathematical Physics*, vol. 32, no. 7, pp. 1847–1853, 1991.